

AD-756 239

INFRARED PHOTOCATHODE RESEARCH

H. Sonnenberg

GTE Sylvania, Incorporated

Prepared for:

Office of Naval Research
Advanced Research Projects Agency

31 December 1972

DISTRIBUTED BY:

NTIS

National Technical Information Service
U. S. DEPARTMENT OF COMMERCE
5285 Port Royal Road, Springfield Va. 22151

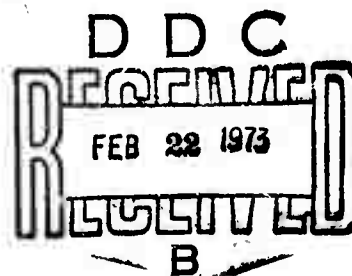
AD 756239

INFRARED PHOTOCATHODE RESEARCH

H. SONNENBERG

GTE SYLVANIA INC.
ELECTRO-OPTICS ORGANIZATION
MOUNTAIN VIEW, CALIFORNIA 94040

FINAL REPORT



DECEMBER 1972

Reproduced by
NATIONAL TECHNICAL
INFORMATION SERVICE
U S Department of Commerce
Springfield VA 22151

PREPARED UNDER CONTRACT N00014-70-C-0079

Details of illustrations in
this document may be better
studied on microfiche

SPONSORED BY

ADVANCED RESEARCH PROJECTS AGENCY
ARPA ORDER NO. 1806

This document has been approved
for public release and sale; its
distribution is unlimited.

UNCLASSIFIED

Security Classification

DOCUMENT CONTROL DATA - R & D

(Security classification of title, body of abstract and indexing annotation must be entered when the overall report is classified)

1. ORIGINATING ACTIVITY (Corporate author) GTE Sylvania Incorporated Mountain View, California 94040		2a. REPORT SECURITY CLASSIFICATION Unclassified	
		2b. GROUP	
3. REPORT TITLE Infrared Photocathode Research			
4. DESCRIPTIVE NOTES (Type of report and inclusive dates) Final Report			
5. AUTHOR(S) (First name, middle initial, last name) Sonnenberg, H.			
6. REPORT DATE Dec. 1972		7a. TOTAL NO. OF PAGES 36	7b. NO. OF REFS
8a. CONTRACT OR GRANT NO. N00014-70-C-0079		9a. ORIGINATOR'S REPORT NUMBER(S)	
b. PROJECT NO.			
c.		9b. OTHER REPORT NO(S) (Any other numbers that may be assigned this report)	
d.			
10. DISTRIBUTION STATEMENT			
11. SUPPLEMENTARY NOTES Details of illustrations in this document may be better studied on microfiche		12. SPONSORING MILITARY ACTIVITY Sponsored by the Advanced Research Projects Agency, and Monitored by the Office of Naval Research	
13. ABSTRACT This report summarizes the results of three years of research on infrared photocathodes. Among the highlights covered by the report are the following: <ul style="list-style-type: none"> (1) Discovery of the most efficient 1.06 micron photocathode, (2) Development of optimum photocathode processing procedures, (3) Quantum yield at 1.3 microns approaching that of the S-1 photosurface at 1.06 microns. (4) Empirical relations between the optimum thickness of Cs₂O low-work-function surface and the wavelength, (5) Empirical relations between the yield and thickness and between the escape probability and thickness of Cs₂O-activated photosurfaces, (6) Heterocathode concept, a new approach to potentially-efficient infrared photoemission, (7) Low-temperature growth of GaAs on Ge by the Gallium-diethyl-chloride technique. 			

14. KEY WORDS	LINK A		LINK B		LINK C	
	ROLE	WT	ROLE	WT	ROLE	WT
(1) Infrared Photocathodes (2) Low Temperature GaAs growth (3) Negative-electron-affinity cathodes (4) Heterocathode (5) Heterojunctions						

II

INFRARED PHOTOCATHODE RESEARCH
FINAL REPORT

31 December 1972

ARPA Order Number: 306/1806
Program Code Number: 00014
Contractor: GTE Sylvania, Inc.
Effective Date: 1 November 1969
Date of Expiration: 31 December 1972
Contract Amount: \$229,183
Contract: N00014-70-C-0079
Project Scientist: Dr. H. Sonnenberg
Telephone: (415) 966-3472
Scientific Officer: Dr. Robert E. Behringer
Title: Infrared Photocathode Research

Sponsored by
Advanced Research Projects Agency
ARPA Order No. 1806

The views and conclusions contained in this document are those of the author and should not be interpreted as necessarily representing the official policies, either expressed or implied, of the Advanced Research Projects Agency or the U.S. Government.

Prepared by

H. Sonnenberg

H. Sonnenberg
Electro-Optics Research and
Development Department

Approved by

L. M. Osterink

L. M. Osterink, Manager
Electro-Optics Research and
Development Department

III

Final Report
 Infrared Photocathode Research
 Contract N00014-70-C-0079

TABLE OF CONTENTS

<u>Section</u>	<u>Title</u>	<u>Page</u>
1.0	Summary	1
2.0	InAsP-Cs ₂ O, A High Efficiency Infrared Photocathode	3
	References	5
2.1	Low-Work-Function-Surface Investigation	6
	References	8
2.2	Long-Wavelength Photoemission from InAs _{1-x} P _x	9
	References	12
2.3	Wavelength Dependence of Optimum Thickness of Cs-O Low-Work-Function Surfaces	13
	References	15
2.4	Effect of Thick Cs-O Layers on Photoemission from Negative-Electron-Affinity Cathodes	17
	References	20
3.0	Concept of the Heterocathode	21
3.1	Materials Growth	24
3.2	Heterojunction Devices	32
	References	36

Section 1.0

INFRARED PHOTOCATHODE RESEARCH

1. SUMMARY

The technical objective of this research was the development of efficient photocathodes for the infrared spectrum, with special emphasis on the 1.5 micron region. The concept of the heterojunction photocathode proposed by us earlier, represented a new approach to the development of an infrared cathode.

This approach, exploited on this contract, led us to the discovery of the most efficient (at that time) 1.06 micron photocathode. Further details of this work are given in Section 2.0 of this report.

Crudely speaking, the response of a negative-electron-affinity-type cathode is either bandgap limited in which case the drop in photoresponse near threshold is directly attributable to the decrease in optical absorption near the bandedge, or it is work-function limited in which case the drop in photoresponse near threshold is due to the influence of a positive potential-barrier near the surface. To attempt to achieve efficient photoemission further into the infrared, smaller-bandgap materials in combination with various low-work-function surfaces were investigated. This work is summarized in Section 2.1.

By far the best results were obtained with Cs-O low-work-function surfaces on InAsP. This work is reported in greater detail in Sections 2.2, 2.3, and 2.4. In Section 2.2, the change in quantum yield with decreasing bandgap is given. The wavelength-dependence of the optimum thickness is given in Section 2.3, and the effect of thick Cs-O layers on photoemission is given in Section 2.4. A simple empirical relationship for the wavelength dependence of the optimum Cs-O thickness is given. Empirical relationships between the yield and thickness and between the escape probability and thickness are also reported.

We have observed photoemission in $\text{InAs}_{0.4}\text{P}_{0.6}$ to 1.45 microns, however the useful response of this cathode extends only to about 1.33 microns. At 1.3 microns we have observed approximately 0.02% quantum efficiency. Note that the response of an S-1 photo-surface at 1.06 microns is about 0.05%. Thus the efficiency of the $\text{InAs}_{0.4}\text{P}_{0.6}$ cathode at 1.3 microns is approaching that of the S-1 at 1.06 microns. We should also emphasize that the response of our $\text{InAs}_{0.4}\text{P}_{0.6}$ is superior to that of the S-1 surface at all wavelengths,

1. (Continued)

particularly in the visible spectrum and again beyond 1.1 microns. However, it is not likely that greater than 0.01% quantum yield can be achieved in InAsP at 1.5 microns by the conventional negative-electron-affinity approach utilizing Cs-O low-work-function surfaces. Consequently, this approach was abandoned and a completely new concept for an infrared photocathode was proposed.

In the new approach, the optical absorption occurs in a small-bandgap semiconductor in intimate contact with a large-bandgap semiconductor known to have a high electron-escape-probability when treated with Cs or Cs and O₂. We have investigated a Ge:GaAs heterojunction. By applying an appropriate bias, photoelectrons excited in the Ge (at 1.5 microns for example) can be injected into the GaAs where they diffuse to the surface and escape into vacuum if a negative-electron-affinity surface is formed. This work, which involves growing thin p-type GaAs layers on Ge substrates is described in greater detail in Section 3. The concept of the heterocathode is discussed in Section 3.0. The growth of GaAs on Ge is discussed in Section 3.1. Noteworthy is the fact that flawless growth could be obtained at 575°C on (111) as well as (100) Ge substrates. The device aspects are discussed in Section 3.2. Good rectification properties of these devices were obtained, but there was insufficient time to make extensive photoemission measurements. In photoemission measurements at zero bias, the GaAs response was obtained, as would be expected. However, it was not possible to make photoemission measurements at non-zero bias since the noise introduced by the bias completely overpowered the signal.

Future work should include an investigation of the noise problem (which may be due to contacts), the heterojunction properties of these devices should be studied further, and extensive internal and external photoemission measurements should be made. It is the author's opinion that photoemission out to 1.5 microns should be achievable by this approach.

Section 2.0

InAsP-Cs₂O, A HIGH-EFFICIENCY INFRARED PHOTOCATHODE

InAsP-Cs₂O, A HIGH-EFFICIENCY INFRARED-PHOTOCATHODE*

H. Sonnenberg

Sylvania Electronic Systems, Electro-Optics Organization, Mountain View, California 94040

(Received 26 January 1970)

The response of an InAs_{0.15}P_{0.85}-Cs₂O photoemitter in the spectral range from 0.4 to 1.1 μ is experimentally investigated. The 0.8% quantum efficiency obtained at 1.06 μ represents more than an order of magnitude improvement in yield over existing S-1 photosurfaces. The physical principle upon which this photoemitter is based is discussed in terms of a simple energy-level diagram.

Until recently the existence of efficient photoemissive surfaces was confined to the visible region of the spectrum. New understanding of the physical processes of photoemission has made possible the design of an infrared photocathode having more than ten times the response of the S-1 photosurface at 1.06 μ. Based on the principle of negative electron-affinity, the new understanding includes the concept of efficient photoemission utilizing a heterojunction consisting of a thin layer of low-electron-affinity *n*-type semiconductor material and a *p*-type semiconductor base.¹ In this paper we use a simple energy-level diagram to explain the physical principle upon which the new photoemitter is based, and discuss our experimental results.

We have investigated photoemission from ultrahigh-vacuum-fractured polycrystalline InAs_{0.15}P_{0.85}-Cs₂O in the spectral range from 0.4 to 1.1 μ. The highest quantum yields yet reported were observed in this emitter. The high efficiency of this cathode can be explained most easily in terms of the simple energy-level diagram shown in Fig. 1.

The emitter owes its high infrared efficiency to the fact that electrons excited even deep within the material can diffuse long distances near the bottom of the conduction band arriving at the edge of the band-bending region of the InAs_{0.15}P_{0.85} with energy above the vacuum level. Except perhaps for the

narrow potential spike at the interface, only a *negative* potential barrier impedes the electron escape into vacuum. If the barrier region is made narrow so that only a small fraction of the electrons escaping across it fall below the vacuum level, efficient electron escape can be obtained.

For our sample of 8.2 × 10¹⁸ cm⁻³, Zn-doped InAs_{0.15}P_{0.85}, the total barrier width, including the Cs₂O layer is about 110 Å. Assuming that the primary energy loss of photoelectrons in the barrier region is through electron-phonon interactions, we calculate that the mean distance an electron in the barrier region can diffuse before falling below the vacuum level is on the order of 70 to 90 Å. It appears that for optimum photoemission, a higher-doped sample is desirable.

Even so, we have observed very efficient infrared

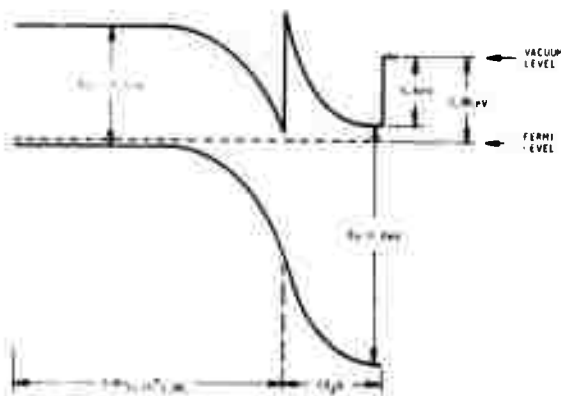


FIG. 1. Simple energy-level diagram of an InAs_{0.15}P_{0.85}-Cs₂O heterojunction photoemitter.

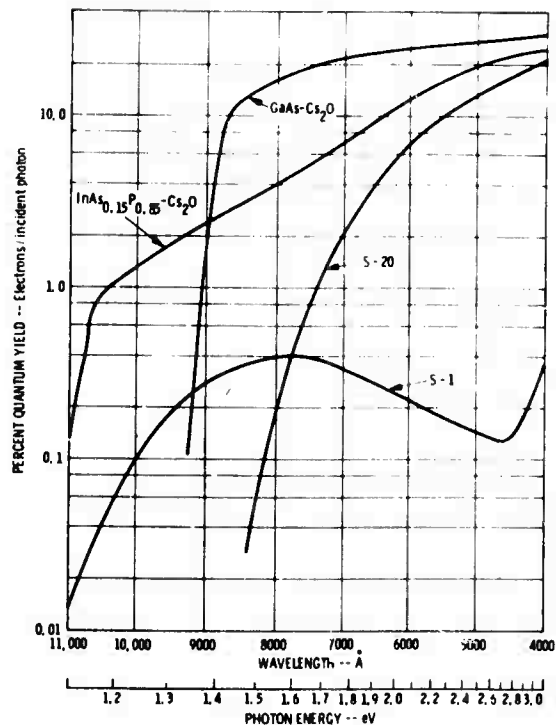


FIG. 2. Spectral response of InAs_{0.15}P_{0.85}-Cs₂O compared to GaAs-Cs₂O, S-20 and S-1 responses.

photoemission in our $\text{InAs}_{0.15}\text{P}_{0.85}\text{-Cs}_2\text{O}$. The spectral response of this photoemitter is shown in Fig. 2, contrasted to the conventional S-1 and S-20 photoresponse, and to another negative-electron-affinity heterojunction photocathode, $\text{GaAs-Cs}_2\text{O}$. The two heterojunction-photocathodes are clearly superior to the conventional ones. $\text{GaAs-Cs}_2\text{O}$ has the best response out to 0.875μ . Beyond 0.9μ , the $\text{InAs}_{0.15}\text{P}_{0.85}\text{-Cs}_2\text{O}$ response is clearly superior to any other photosurface. Note that at 1.06μ the quantum efficiency is 0.8%. This is more than 20 times that of the S-1 photocathode at this wavelength. Even at 1.1μ , the quantum yield is in excess of 0.1%. The sharp drop in quantum yield near 1.06μ in $\text{InAs}_{0.15}\text{P}_{0.85}\text{-Cs}_2\text{O}$ and 0.875μ in $\text{GaAs-Cs}_2\text{O}$ reflects the decrease in optical absorption near the band-edge of the respective materials. It appears that efficient response even further into the infrared may be obtained in $\text{InAsP-Cs}_2\text{O}$ by going to still lower bandgap material.

The quantum yield was measured using a grating monochromator with a spectral width of $\pm 60 \text{ \AA}$, doubly filtered to eliminate higher-order light. The response at 1.06 and at 0.6328μ was con-

firmed with a Nd:YAG laser and a He:Ne laser, respectively, and was found to be within 15% of that obtained with the monochromator. The Eppley thermopile used as a standard in our calibrations has a nominal absolute accuracy of $\pm 5\%$. This was verified with two other thermopiles.

To our knowledge, 0.8% quantum yield at 1.06μ is the highest yield yet reported. We have repeatedly obtained 0.8% quantum efficiency and are confident that it will be possible to obtain in excess of 1% quantum yield at 1.06μ in improved InAsP material. Clearly, this cathode could find important application in efficient Nd:YAG laser light detection.

The author would like to thank A. G. Thompson and J. W. Wagner of Beil and Howell for the material.

*This research was supported in part by the Advanced Research Projects Agency of the Department of Defense and was monitored by the Office of Naval Research under contract No. N00014-70-C-0079.

¹H. Sonnenberg, *Appl. Phys. Letters* **14**, 289 (1969).

Section 2.1

Low-Work-Function-Surface Investigations

2.1 LOW-WORK-FUNCTION-SURFACE INVESTIGATIONS

The major small-bandgap materials investigated were Ge, GaSb, InAs_{0.25}P_{0.75} and InAs_{0.4}P_{0.6}. In an attempt to establish a negative-electron-affinity condition in these small-bandgap materials, a number of different low-work-function surfaces, including n-Cs₃Sb, Ag-Cs₂O, and Cs₂O were investigated.

Because of its low electron-affinity, Cs₃Sb is a potential low-work-function surface.⁽¹⁾ In order to attempt to grow stoichiometric n-Cs₃Sb low-work-function surfaces, different processing techniques were employed: Cs-Sb films were formed in ultrahigh vacuum at room temperature, at 100°C, at 150°C and 200°C by coevaporating Cs and Sb in the presence of excess Cs vapor; alternate layers of Cs and Sb reacted at different temperatures were investigated; Cs-Sb layers in conjunction with Cs₂O layers were also investigated. By far the best results were obtained when Cs₂O only was used. This may mean that the height of the interfacial barrier for Cs-Sb processing is much greater than that associated with Cs-O processing.

We have also investigated Ag-Cs₂O low-work-function surfaces. There is evidence that Ag-Cs₂O forms low-work-function surfaces⁽²⁾ (as low as 0.6 eV). Consequently if a monolayer of Ag is sandwiched between a small-bandgap material and the Cs₂O, lower-work-function surfaces may form. We have investigated the effect of Ag on photoemission from InAs_{0.25}P_{0.75}, and have come to the following conclusions:

- (1) Photoemission from InAs_{0.25}P_{0.75}-Cs₂O is not influenced greatly by thin layers of Ag.
- (2) In all cases the efficiency of the photosurface was decreased by the addition of Ag.
- (3) Threshold response is more greatly affected than the visible response.
- (4) The dependence of the quantum efficiency on the thickness of the Ag layer is exponential over at least one order of magnitude.
- (5) From Fowler plots we determined that the work function (interfacial barrier height) is not affected noticeably by the Ag film.

Since in all cases the best results have been obtained with Cs₂O only, subsequent efforts were concentrated on improving the processing of the Cs₂O low-work-function surface. From Fowler plots of our InAs_{0.25}P_{0.75}-Cs₂O data, we found that the interfacial-barrier height remained constant to within ±0.05 eV independent of the Cs-O surface treatment.

2.1 (Continued)

For example, the same barrier height was formed whether Cs and O₂ were simultaneously deposited on the surface, or Cs and O₂ were alternately cycled to form the low-work-function surface. This consistency in the interfacial-barrier height, in spite of substantial differences in the quantum yield led to the conclusion that for identical absorbing materials, fluctuations from cathode to cathode, in the quantum yield result largely from differences in the thickness of the low-work-function surface required to achieve optimum photoemission.

Accordingly, we have developed a Cs-O processing technique which consistently gives optimum photoemission at minimum thickness. The essential features of this technique are as follows:

- (1) Cs is deposited onto the semiconductor surface at a given rate until the photoemission response is approximately optimized.
- (2) Maintaining this set Cs rate, O₂ is introduced simultaneously at an exposure level such that the rate of increase in photoemission from the cathode is maximized.

The philosophy behind the technique is that for a given rate of Cs exposure, the O₂ exposure is adjusted to give a maximum rate of increase in photoemission in order to minimize the thickness of the low-work-function surface. This in turn maximizes the escape probability, and thereby optimizes the photoresponse.

(1) H. Sonnenberg, Appl. Phys. Lett. 14, 289 (1969)

(2) W. E. Spicer, Private communication.

Section 2.2

Long-Wavelength Photoemission from $\text{InAs}_{1-x}\text{P}_x$

Long-Wavelength Photoemission from $\text{InAs}_{1-x}\text{P}_x$

H. Sonnenberg

GTE Sylvania Inc., Electro-Optics Organization, Mountain View, California 94040

(Received 19 August 1971)

Efficient photoemission from $\text{InAs}_{1-x}\text{P}_x$ (Cs-O) with a band-gap-limited threshold at 1.4μ was observed. Indirect measurements of the composition and thickness of the Cs-O low-work-function surface suggest that the surface consists of about one monolayer of Cs, followed by approximately one monolayer of cesium oxide. These data make an interpretation of the low-work-function properties of Cs-O in terms of the heterojunction model (based on the bulk properties of Cs_2O) questionable.

In early 1970 we reported¹ the discovery of the $\text{InAs}_{1-x}\text{P}_x$ photocathode, which at the time was the most efficient $1.06\text{-}\mu$ photoemitter yet developed. Since then, James *et al.*² have achieved even higher quantum yields at 1.06μ in better quality $\text{InAs}_{1-x}\text{P}_x$. Comparable results were reported by Fisher *et al.*³ in $\text{Ga}_{1-x}\text{In}_x\text{As}$. In each case, the photocathode surface was treated with Cs and O_2 to lower the work function of the cathode material to establish a negative-electron-affinity condition. Although the experimental results reported by different investigators have been roughly comparable, the function of the Cs and O_2 in lowering the work function of the photocathode material has recently been the subject of considerable controversy. On the one hand is the interpretation in terms of the heterojunction model^{4,5} which ascribes bulk properties to a Cs_2O layer assumed to be present in the low-work-function surface. On the other hand is the interpretation in terms of a surface dipole layer of Cs and O_2 .^{3,6} This letter will no doubt add to the controversy by presenting results on the long-wavelength response of $\text{InAs}_{1-x}\text{P}_x$ photocathodes, and reporting on indirect measurements of the thickness and composition of the Cs-O low-work-function surface.

The infrared photoresponse of three different $\text{InAs}_{1-x}\text{P}_x$ photocathodes is shown in Fig. 1. Curve 1 is repeated from Ref. 1 and curves 2 and 3 represent our more recent results on $\text{InAs}_{0.25}\text{P}_{0.75}$ and $\text{InAs}_{0.4}\text{P}_{0.6}$, respectively. Curve 3 is of most interest since it shows relatively efficient band-gap-limited photoemission out to 1.4μ . In the past, we have attempted to explain our results in terms of the heterojunction model, the validity of which has now been questioned.^{3,6}

The major objection to the heterojunction model was raised by direct chemical analysis⁶ of the Cs content of GaAs (Cs) and GaAs (Cs-O) photocathodes. It was shown that if Cs_2O is formed at all, peak sensitivity is reached with the equivalent of one monolayer of Cs and one monolayer of Cs_2O . Clearly, the Cs-O low-work-function-surface properties are difficult to explain with a model based on the bulk properties of Cs_2O when only one monolayer of Cs_2O is present.

We have indirectly measured the thickness of the Cs-O low-work-function surface on $\text{InAs}_{1-x}\text{P}_x$ by a different technique and find, in agreement with Sommer *et al.*,⁶ that the Cs-O layers may be sufficiently thin to make the heterojunction interpretation ques-

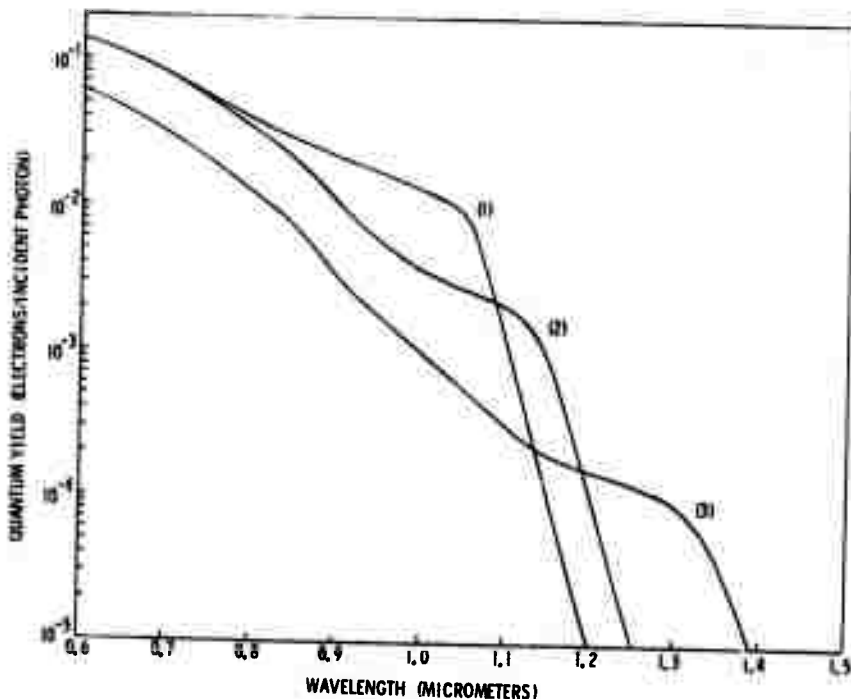


FIG. 1. Quantum yield of $\text{InAs}_{1-x}\text{P}_x$ treated with (Cs-O) low-work-function surfaces for $x=0.85$, $x=0.75$, and $x=0.6$, curves 1-3, respectively.

TABLE. I. Ratio of Cs to O₂ and Cs-O low-work-function coverage for InAs_{0.25}P_{0.75} optimized at 6328 and 10 000 Å. The factor Y is a constant multiplier (Ref. 7).

Sample number	Ratio ^a Cs/O		Ratio ^b Cs/O		Coverage ^b (monolayers)	
	Cs/O		Cs/O			
	0. 6328 opt	1. 0 opt	0. 6328 opt	1. 0 opt	0. 6328 opt	1. 0 opt
1	(0.77)Y	(0.67)Y	(0.47)Y	(0.51)Y	(1)Cs+	(1)Cs+
2	(0.78)Y	(0.82)Y	(0.51)Y	(0.63)Y	(0.7)Cs ₂ O	(1.4)Cs ₂ O
3	(0.74)Y	(0.66)Y	(0.49)Y	(0.52)Y	(1)Cs+	(1)Cs+
4	(0.69)Y	(0.67)Y	(0.48)Y	(0.51)Y	(0.8)Cs ₂ O	(1.6)Cs ₂ O
					(1)Cs+	(1)Cs+
					(0.9)Cs ₂ O	(1.4)Cs ₂ O

^aAssuming all Cs is converted to oxide.

^bAssuming one monolayer of Cs is not converted.

tionable. The thickness was estimated as follows: The Cs generation rate was first stabilized. Next, the InAs_{1-x}P_x crystal was cleaved and the time taken to optimize the surface with Cs only recorded. Maintaining this set Cs rate, O₂ was then introduced simultaneously at an exposure level such that the rate of increase in photoemission from the cathode was maximized. The total O₂ exposure was measured with an Ultek Partial Pressure Analyzer by integrating over the exposure period. To determine the total Cs and O₂ exposure, we assume that the Cs and O₂ sticking coefficients do not change significantly with coverage.

Sensitization of electron-affinity photocathodes by the simultaneous exposure to Cs and O₂ described above differs from the standard method which involves the alternate application of Cs and O₂. We have been using the simultaneous-exposure technique for a number of years now and find that in our work, this method gives better results, particularly with smaller-band-gap materials. The philosophy behind the technique is that for a given rate of Cs exposure, the O₂ exposure should be adjusted to give a maximum rate of increase in photoemission in order to

minimize the thickness of the low-work-function surface. This in turn would maximize the escape probability, and thereby optimize the photoresponse.

It seems likely that at least part of the controversy over Cs-O low-work-function surfaces is due to differences in the processing technique. In our work the simultaneous technique was used exclusively.

Table I summarizes our findings for InAs_{0.25}P_{0.75}. The first two columns of data give the ratio of Cs to O₂ assuming that all Cs is converted to oxide.⁷ The first column gives the ratio of Cs to O₂ for the case in which the photoresponse is optimized at 6328 Å, and the second column gives the ratio for the case in which the photoresponse is optimized at 10 000 Å. If a stoichiometric Cs-O compound is formed,⁸ then this ratio should remain constant. The ratio does not remain constant. However, the ratio of Cs to O₂ given in the next two columns, where it is assumed that one monolayer⁹ of Cs is not converted to oxide, remains relatively constant, suggesting that our Cs-O low-work-function surfaces consist of a Cs layer and an oxide layer, the Cs layer being slightly less than a monolayer thick.⁹ If we assume that the

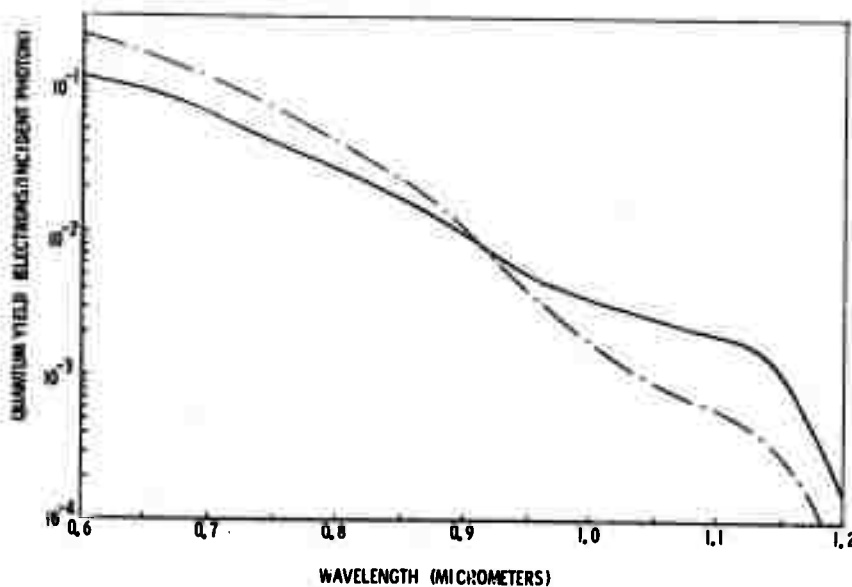


FIG. 2. Quantum yield of InAs_{0.25}P_{0.75} optimized at 6328 Å (broken curve) compared to the yield obtained on the same sample when the processing is continued until the yield at 10 000 Å is optimized (solid curve).

oxide is Cs_2O , then the thickness of the low-work-function layer can be estimated from the Cs exposure and the relative bulk densities of the Cs_2O and of the Cs and Cs_2O are given in the last two columns.

The photoyield in the visible (6328 Å) is optimized with a coverage of only about one monolayer of Cs and 0.8 monolayers of Cs_2O . This case should correspond most closely to the coverage required for GaAs and is in excellent agreement with the findings of Sommer *et al.*⁶ for GaAs. However, when the photoyield is optimized at 10 000 Å the coverage increases to approximately 1 monolayer of Cs and 1.4 monolayers of Cs_2O . Apparently, thicker cesium oxide coverage is necessary to optimize the photoresponse of smaller-band-gap materials. This is in contrast to the claim made in Ref. 3.

Figure 2 shows the effect of the thicker oxide layer on the photoresponse of sample number 1. The response in the visible spectrum decreases, whereas the threshold response increases. The decrease in the response is likely the result of increased electron scattering in the thicker oxide layer, and the increase in the infrared yield is probably associated with a decrease in the work function of the Cs-O surface which more than compensates for the increased scattering in the thicker layer.

Subject to the assumptions implied in this paper, the following conclusions can be reached: (1) Relatively efficient photoemission with a band-gap-limited threshold at 1.4μ can be achieved in $\text{InAs}_{1-x}\text{P}_x$. (2) The low-work-function Cs-O surface probably consists of a Cs layer slightly less than a monolayer thick, followed by an oxide layer of monolayer dimensions. (3) For optimum infrared response, small-band-gap materials require thicker oxide coatings than do larger-band-gap materials.

The fact that relatively efficient photoemission was observed with a band-gap-limited threshold at 1.4μ

shows that earlier predictions¹⁰ of the long-wavelength limit of Cs-O covered photocathodes have overemphasized the influence of the interfacial barrier (if it exists). Furthermore, since the thickness of the Cs-O low-work-function surface appears to be of monolayer proportions, the concept of the heterojunction cathode^{4,5} based on the bulk properties of Cs_2O if used at all must be used with caution. However, in contrast to a previous interpretation of band-gap-limited photoemission out to 1.3μ ,³ it can be shown¹¹ that band-gap-limited photoemission out to 1.4μ can be taken neither as evidence for the absence of an interfacial barrier, nor evidence for an interfacial-barrier height less than 0.89 eV.

¹Research supported by the Advanced Research Projects Agency of the Department of Defense and monitored by the Office of Naval Research under Contract No. N00014-70-C-0079.

²H. Sonnenberg, Appl. Phys. Letters 16, 245 (1970).

³L.W. James, G.A. Antypas, J.J. Uebbing, T.O. Ycp, and R.L. Bell, J. Appl. Phys. 42, 580 (1971).

⁴D.G. Fisher, R.E. Enstrom, and B.F. Williams, Appl. Phys. Letters 18, 371 (1971).

⁵H. Sonnenberg, Appl. Phys. Letters 14, 289 (1969).

⁶J.J. Uebbing and L.W. James, J. Appl. Phys. 41, 4505, (1970).

⁷A.H. Sommer, H.H. Whitaker, and B.F. Williams, Appl. Phys. Letters 17, 273 (1970).

⁸The ratio purposely contains a constant multiplier Y to reflect the fact that we do not know the absolute calibration of our partial-pressure analyzer, and furthermore to account for the large discrepancy in the literature as to the Cs coverage required for optimum yield. For example, S. Garbe [Solid State Electron 12, 893 (1969)] measures 3×10^{14} Cs/cm² for GaAs and T.E. Fischer [Phys. Rev. 142, 519 (1966)] measures 1×10^{15} Cs/cm² for InP.

⁹A monolayer of Cs is arbitrarily defined as the coverage required to optimize the photoresponse with Cs only.

¹⁰Experiments with much thicker Cs-O films confirm that the ratio remains constant when it is assumed that slightly less than a monolayer of Cs remains unconverted.

¹¹L.W. James and J.J. Uebbing, Appl. Phys. Letters 16, 370 (1970).

¹²J.D. Tynal and H. Sonnenberg (unpublished).

Section 2.3

Wavelength Dependence of Optimum Thickness of Cs-O Low-Work-Function Surfaces

Wavelength dependence of optimum thickness of Cs-O low-work-function surfaces*

H. Sonnenberg

GTE Sylvania, Incorporated, Electro-Optics Organization, Mountain View, California 94040

(Received 5 April 1972)

The amount of Cs-O low-work-function surface material required to optimize the photoresponse of $\text{InAs}_{0.4}\text{P}_{0.6}$ depends upon the wavelength at which the response is to be maximized. It is shown that the optimum thickness increases exponentially with wavelength.

In the Cs-O processing of negative-electron-affinity infrared photocathodes, one commonly finds that the photoresponse in the visible spectrum peaks earlier than the infrared response. Continued processing, beyond that required to optimize the visible response, generally leads to continued improvement in the infrared response but at the expense of the response in the visible.¹ Thus for a given infrared cathode, different thicknesses of Cs-O low-work-function material are required to optimize the photoresponse at different wavelengths. We have investigated this behavior in detail for $\text{InAs}_{0.4}\text{P}_{0.6}$ - (Cs-O) and report here a very simple empirical relationship between optimum thickness and wavelength.

$\text{InAs}_{0.4}\text{P}_{0.6}$ with a band gap less than 1 eV was chosen since its useful photoresponse extends over a broad spectral range to 1.3 μ . The yield curves for different levels of Cs and O_2 exposure were directly recorded with a phase-sensitive detection apparatus and a Perkin-Elmer E-1 scanning monochromator. A complete scan from 0.45 to 1.4 μ takes about 15 min.

The photoresponse of the $\text{InAs}_{0.4}\text{P}_{0.6}$ cathode with one monolayer of Cs² on the surface was first recorded. The simultaneous-exposure technique¹ was then used to process the cathode with Cs and O_2 in approximately one-monolayer-of-Cs steps. The photoresponse at the end of each step was recorded. To avoid Cs loss from the cathode between processing steps, the Cs channel, rather than being turned off completely, was turned down so that the arrival rate of Cs atoms at the cathode surface was in equilibrium with the loss rate. Stability in the photoresponse at each exposure level could easily be maintained this way.

To investigate the effect of increasing Cs-O coverage on the photoresponse of the cathode, the yield was plotted as a function of Cs exposure for different wavelengths as shown in Fig. 1. Each vertical set of points represents the photoresponse of the cathode at that particular level of Cs and O_2 exposure. The first set of points (at 1.0 monolayer) is for Cs alone, and subsequent sets of points are for increasing Cs-O exposure, measured in terms of Cs monolayers.

Figure 1 clearly shows that different thicknesses of Cs-O layers are required to optimize the photoresponse at different wavelengths. For example, the photoresponse at 4500 Å is optimized by a coverage of only about 2.2 monolayers of Cs, whereas the photoresponse at 10 500 Å is not optimized until the coverage has grown to approximately 4.2 monolayers of Cs.³

The thickness corresponding to the maximum photoresponse (optimum thickness) at the different wavelengths is plotted in Fig. 2 as a function of wavelength. The data from 0.45 to 1.1 μ are taken from the position of the maxima of the parametric curves of Fig. 1, whereas the data at 1.3 μ are taken from a number of different experiments where the processing was not interrupted until the response at 1.3 μ was optimized.

It appears from Fig. 2 that the amount t of Cs-O (measured in monolayers of Cs) required to optimize the photoresponse is exponentially dependent on the wavelength λ (μ), i. e.,

$$t \approx T e^{\beta \lambda}. \quad (1)$$

For this particular experiment, $T = 1.4$ monolayers of Cs⁴ and $\beta = 1.02 \mu^{-1}$.

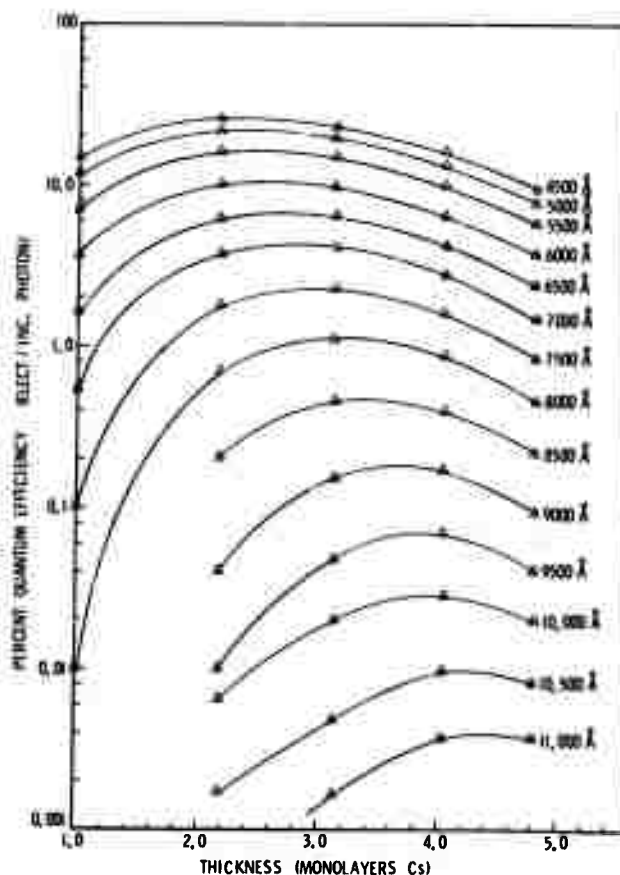


FIG. 1. Quantum efficiency as a function of Cs-O low-work-function surface thickness measured in monolayers of Cs with wavelength as a parameter.

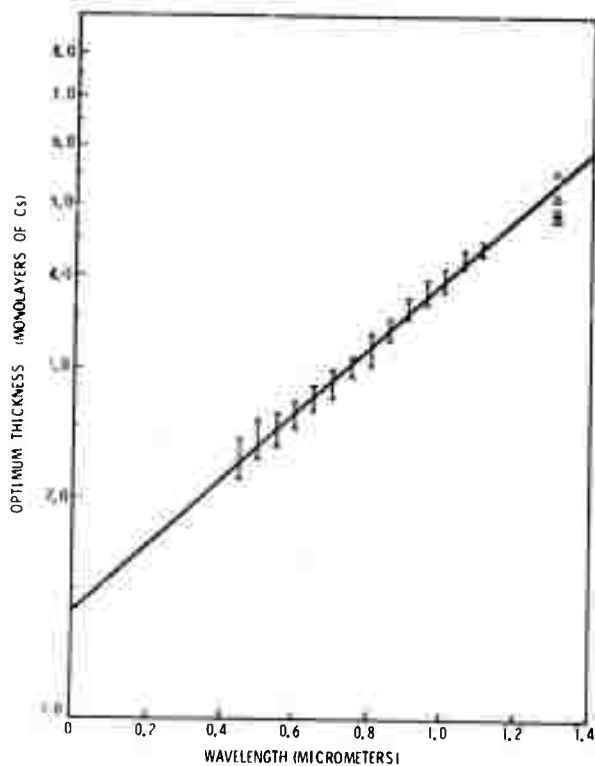


FIG. 2. Thickness of Cs-O low-work-function surface required to maximize the photoresponse of $\text{InAs}_{0.4}\text{P}_{0.6}$ as a function of wavelength.

It is not immediately apparent why the optimum thickness and the wavelength are related by a simple exponential, but the fact that thicker oxide layers are required to optimize the photoresponse in the infrared than in the visible can be understood in terms of the electron scattering and the change in work function of the oxide surface. The work function of the surface decreases with increasing oxide thickness. Counteracting this effect is the increased electron scattering in thicker oxide layers. At high photon energies, a much larger fraction of excited carriers reaches the interface with sufficient energy to escape into vacuum than at low photon energies. Consequently, the effect of reducing the work function is much more pronounced for the threshold response than for the short-wavelength response. Hence, the optimum balance between electron scattering and reduction in work function of the surface is reached more quickly for the high-energy electrons than for the low-energy electrons, and the optimum thickness increases with increasing wavelength.

We have confirmed the exponential dependence for *continuously* processed cathodes as well. We find in general, however, that thinner Cs-O coverage is required to optimize the photoresponse of continuously processed cathodes, as demonstrated in Fig. 2, and that the overall photoresponse of these cathodes is much better than that of cathodes for which the processing is interrupted. To underscore this, compare the yield curve shown in Fig. 3 with the data at 4.8 monolayers shown in Fig. 1. Figure 3 shows the spectral response⁵ of the cathode

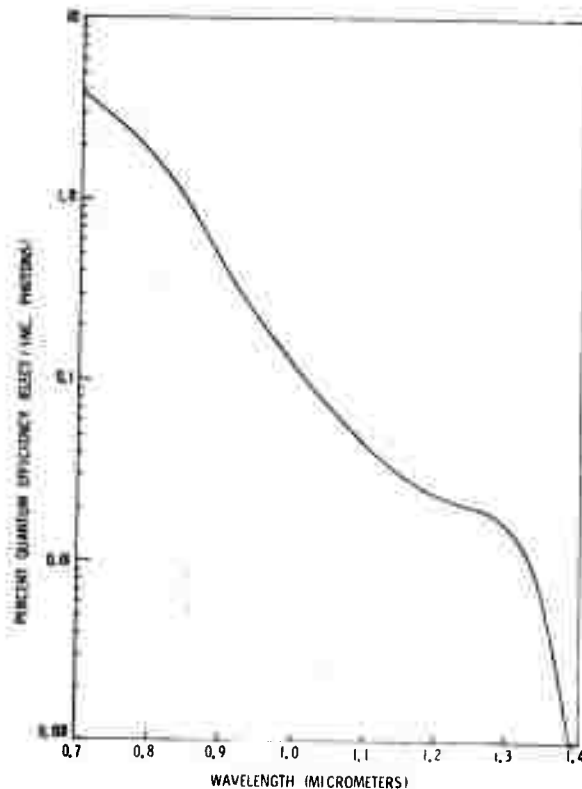


FIG. 3. Quantum yield of continuously processed $\text{InAs}_{0.4}\text{P}_{0.6} - (\text{Cs-O})$.

represented by the point in Fig. 2 at 1.3μ and 4.9 monolayers of Cs.⁶

One may well ask whether the exponential relationship given by Eq. (1) is applicable only to $\text{InAs}_{0.4}\text{P}_{0.6}$ or if it is more universally applicable. Although we have not *specifically* attempted to determine the wavelength dependence of the optimum thickness for $\text{InAs}_{0.25}\text{P}_{0.75}$, the data that we do have are in agreement with Eq. (1). We have also attempted to verify Eq. (1) for GaAs. The parametric curves (comparable with those of Fig. 1) exhibit a very broad maximum that makes interpretation difficult. If the optimum thickness for GaAs is exponentially dependent on the wavelength, its β must be very small. It may be, however, that Eq. (1), and this is purely conjecture, is applicable only to cathodes in which the top of the interfacial barrier is above the bottom of the conduction band.

*Research supported by the Advanced Research Projects Agency of the Department of Defense and monitored by the Office of Naval Research under Contract No. N00014-70-C-0079.

¹H. Sonnenberg, Appl. Phys. Letters 19, 431 (1971).

²A monolayer of Cs is defined here as the amount of Cs required to optimize the photoresponse at 6328 \AA with Cs alone. For GaAs, S. Garbe [Solid-State Electron. 12, 893 (1969)] measured $3 \times 10^{14} \text{ Cs/cm}^2$ for optimum Cs coverage, and J. J. Uebbing and L. W. James [J. Appl. Phys. 41, 4505 (1970)] measured $5.6 \times 10^{14} \text{ Cs/cm}^2$. Giving equal weight to these measurements, we determine a mean-optimum Cs

coverage of 4.3 Cs/cm^2 . This is equivalent (within experimental accuracy) to one monolayer of Cs since there are $4.43 \times 10^{14}/\text{cm}^2$ unit cells on the surface.

³We assume that the Cs and O_2 sticking coefficients do not change significantly with coverage.

⁴The fact that T is greater than 1 shows that some O_2 is required to optimize the photoresponse at all wavelengths,

including the ultraviolet range.

⁵Note that the efficiency at 1.3μ is almost 0.02%. Further improvement with better $\text{InAs}_{0.4}\text{P}_{0.6}$ material can be expected.

⁶If we make the same assumptions about the Cs-O surface that were made in Ref. 1, we find that the low-work-function surface consists of approximately one monolayer of Cs and 1.7 monolayers of Cs_2O .

Section 2.4

Effect of Thick Cs-O Layers on Photoemission from Negative-Electron-Affinity Cathodes

Effect of thick Cs-O layers on photoemission from negative-electron-affinity cathodes*

H. Sonnenberg

GTE Sylvania, Incorporated, Electro-Optics Organization, P.O. Box 188
Mountain View, California 94040

(Received 8 May 1972; in final form 19 July 1972)

The effect of thick Cs-O layers on photoemission from GaAs and $\text{InAs}_{0.4}\text{P}_{0.6}$ cathodes is experimentally investigated. Simple empirical relationships between the yield and thickness and between the escape probability and thickness are given.

The efficiency of small-band-gap negative-electron-affinity (NEA) cathodes near threshold is much less than the efficiency near threshold of larger-band-gap materials. For example, the yield of $\text{InAs}_{0.4}\text{P}_{0.6}$ at 1.3μ is only about 10^{-3} that of GaAs at 0.85μ . The major cause for this difference has been correctly identified as being due to interfacial barrier effects.^{1,2} However, since thicker cesium-oxide coverage is required to optimize the photoresponse of smaller-band-gap materials,³ part of the difference in threshold yield should be due to this difference in thickness. We have investigated the effect of thick Cs-O layers on photoemission from NEA cathodes and show that a substantial decrease in yield may be expected on the basis of the difference in thickness alone. A simple empirical relation giving the effect of thick Cs-O layers on photoemission is obtained.

The yield data were directly recorded with an analog recording system which included a phase-sensitive de-

tection apparatus and a scanning monochromator. The O_2 exposure was recorded with a partial-pressure analyzer and was used as a check on the Cs coverage,⁴ which was estimated by timing the exposure periods as described in Ref. 3. Photoemission measurements were made on GaAs and $\text{InAs}_{0.4}\text{P}_{0.6}$ sensitized with Cs and O_2 by the simultaneous-exposure technique.³

The spectral response with the infrared yield optimized was first recorded. Additional yield curves were then recorded for increasing Cs and O_2 coverage. To avoid Cs loss from the cathode between processing steps, the Cs channel was turned down so that the arrival rate of Cs atoms at the cathode was in equilibrium with the loss rate. The point of equilibrium was estimated from the stability of the photoresponse and remained essentially the same at all exposure levels.

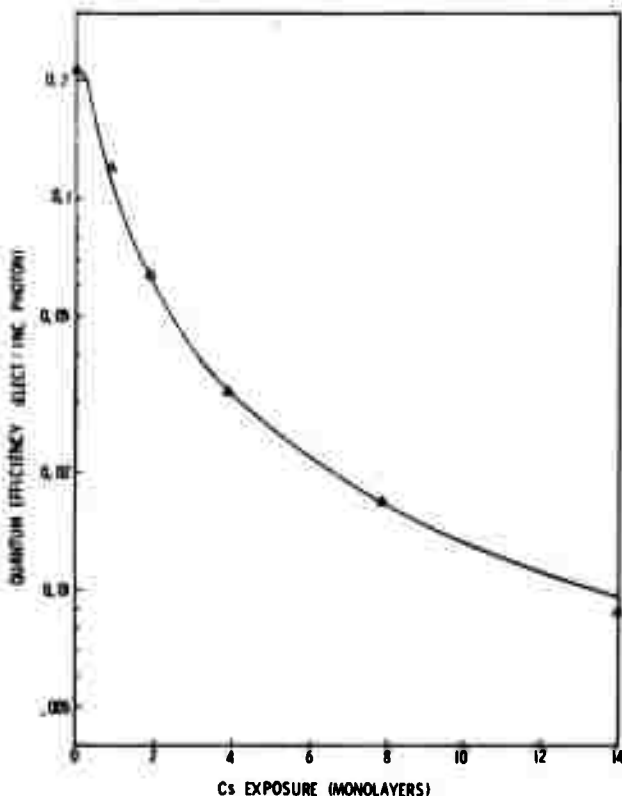


FIG. 1. Thickness dependence of the quantum efficiency η of GaAs at 7500 \AA . The points represent the experimental data, and the solid curve is a plot of the equation $\eta = 0.213 \times [1 - \exp(-0.65/t)]$.

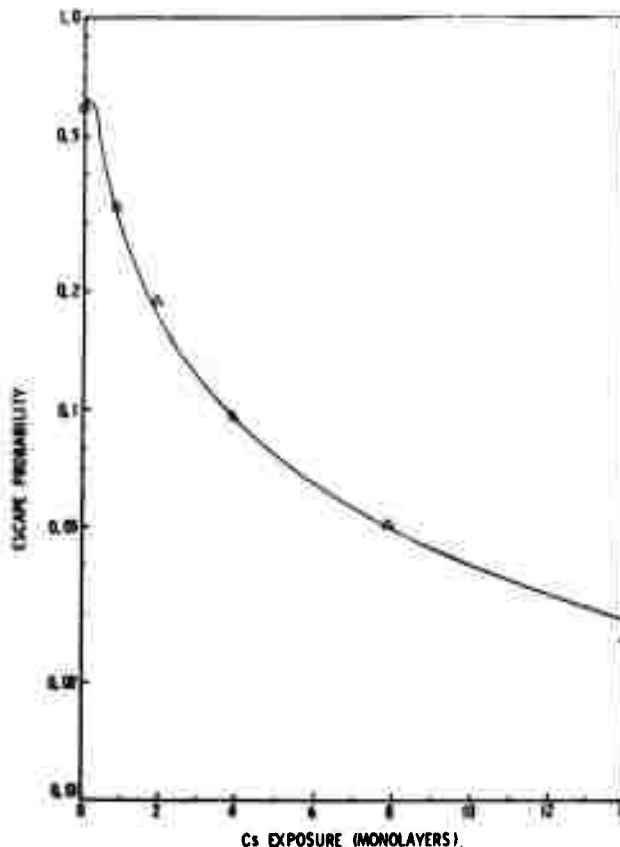


FIG. 2. Thickness dependence of the escape probability P of GaAs at 7500 \AA . The points represent the experimental data, and the solid curve is a plot of the equation $P = 0.63 \times [1 - \exp(-0.65/t)]$.

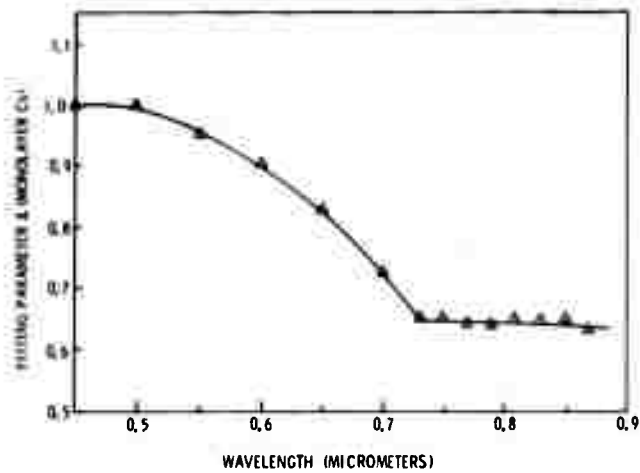


FIG. 3. Wavelength dependence of the fitting parameter for Cs-O low-work-function surfaces on GaAs.

The quantum efficiency of GaAs at 7500 Å is shown in Fig. 1 as a function of thickness measured in monolayers⁵ of Cs. The points represent the experimental values and the solid curve represents the equation

$$\eta = \eta_0(1 - e^{-t/l}), \quad (1)$$

where η is the quantum efficiency (electrons/incident photon) as a function of thickness t (monolayers of Cs), η_0 is the peak quantum efficiency (0.213 electrons/incident photon for the curve shown), and l (0.65 monolayers of Cs for the curve shown) is a fitting parameter. The thickness l does not represent the total coverage but rather the coverage *beyond* that required to optimize the infrared photoresponse. The total coverage is given by $t = l + t_0$, where t_0 is the coverage required to optimize the infrared response. Note that Eq. (1) satisfies the requirement of zero slope at the origin ($t = 0$). This is a necessary requirement since the origin is chosen at optimum coverage.

Near threshold, the yield of III-V NEA cathodes is given by⁶

$$\eta = P(1 - R)F[1 + (1/\alpha L)]^{-1}, \quad (2)$$

where the symbols used have the usual meaning. The factor $F[1 + (1/\alpha L)]^{-1}$, which accounts for the generation and transport of the photoelectrons in the III-V semiconductor, clearly does not change with surface treatment. For the Cs-O layer thicknesses considered here, we can probably safely assume that the reflectivity R of the surface remains that of clean GaAs. This leaves only the escape probability P dependent on surface treatment, which must therefore mirror the thickness dependence of η , i.e.,

$$P = P_0(1 - e^{-t/l}), \quad (3)$$

where P_0 is the escape probability at $t = 0$. A similar argument will quickly show that Eq. (3) should be valid not only near threshold, but over the entire spectral range of response of the III-V NEA cathode.

To verify Eq. (3) experimentally, we have made a least-squares-fit analysis of Eq. (2) and our yield data at each

exposure level to determine $P(t)$. The points given in Fig. 2 represent the escape probabilities at 7500 Å obtained from the least-squares-fit analysis, and the solid curve represents Eq. (3) with the escape probability⁷ $P_0 = 0.63$ and a fitting parameter $l = 0.65$ monolayers of Cs. As expected, the same fitting parameter used to fit the data in Fig. 1 describes the data in Fig. 2. Equation (3) with $P_0 = 0.57$ and $l \approx 10$ "layers of Cs-O" is also in reasonable agreement with the estimated X-electron-escape probability given in Fig. 8 of Ref. 8.

The fitting parameter l is not constant, however, and Fig. 3 shows its wavelength dependence. For the Γ electrons, l is approximately constant at 0.65 monolayers of Cs. We would expect a constant l for this case since most of the photoelectrons arriving at the surface have thermalized in the Γ -conduction-band minimum. At shorter wavelengths, l increases and appears to saturate at about 1.0 monolayer of Cs.

We have also verified Eq. (1) for $\text{InAs}_{0.4}\text{P}_{0.6}$. Figure 4 shows the thickness dependence of the yield from $\text{InAs}_{0.4}\text{P}_{0.6}$ at 6300 Å (upper curve) and 7000 Å (lower curve). The points on the curves are the actual data points, and the solid line represents Eq. (1) with $\eta_0 = 0.062$ and $l = 0.6$ for the upper curve, and $\eta_0 = 0.0335$ and $l = 0.5$ for the lower curve.

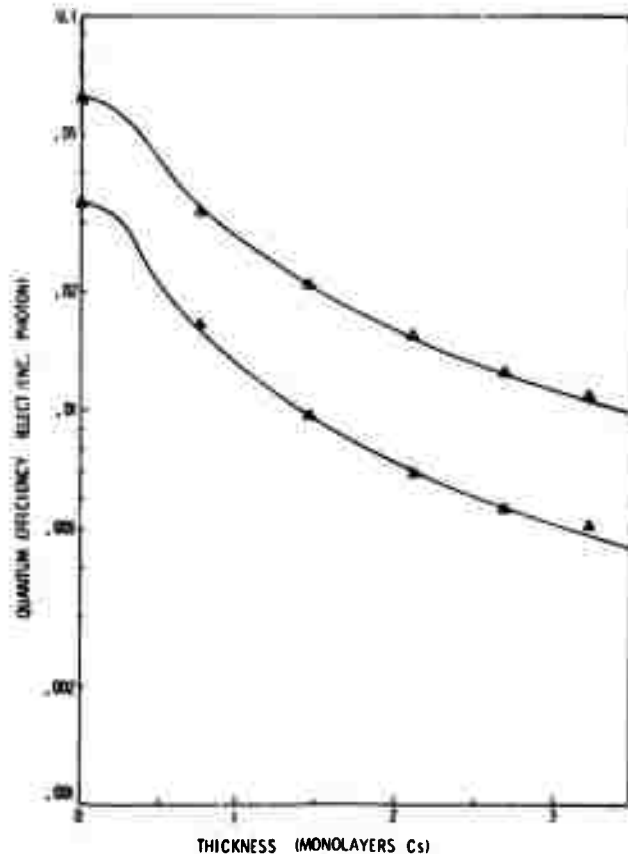


FIG. 4. Thickness dependence of the quantum efficiency η of $\text{InAs}_{0.4}\text{P}_{0.6}$ at 6300 Å (upper curve) and 7000 Å (lower curve). The points represent the experimental data, and the solid curves are plots of the equations $\eta = 0.062[1 - \exp(-0.6/t)]$ and $\eta = 0.0335[1 - \exp(-0.5/t)]$ for the upper and lower curves, respectively.

If, as in Ref. 3, we assume that the sticking coefficient of Cs on $\text{InAs}_{0.4}\text{P}_{0.6}$ and on GaAs does not change significantly with coverage,⁹ then the Cs-O low-work-function surface in an infrared-optimized $\text{InAs}_{0.4}\text{P}_{0.6}$ cathode is approximately 2.3 monolayers of Cs thicker than that of optimized GaAs. From Eq. (1), with $l = 0.65$ monolayers we find that an additional 2.3 monolayers of Cs would reduce the infrared photoresponse of GaAs by a factor of about 4. We do not have sufficient data on $\text{InAs}_{0.4}\text{P}_{0.6}$ to allow us to determine its fitting parameter near threshold; however, from Fig. 4 we expect that it will be smaller than 0.65 monolayers. Consequently, alone on the basis of the increased thickness required to optimize the infrared response of $\text{InAs}_{0.4}\text{P}_{0.6}$, we would expect the threshold response of $\text{InAs}_{0.4}\text{P}_{0.6}$ to be lower than that of GaAs by a factor of 5 or more.¹⁰

*Research supported by the Advanced Research Projects Agency of the Department of Defense and monitored by the Office of Naval Research under Contract No. N00014-70-C-0679.

¹L. W. James and J. J. Uebbing, *Appl. Phys. Letters* 16, 370 (1970).

²R. L. Bell, L. W. James, G. A. Antypas, J. Edgecumbe, and R. L. Moon, *Appl. Phys. Letters* 19, 513 (1971).

³H. Sonnenberg, *Appl. Phys. Letters* 19, 431 (1971).

⁴The ratio of Cs to O₂ remains constant.

⁵A monolayer of Cs is defined here as the amount of Cs required to optimize the photoresponse at 6328 Å with Cs alone. For GaAs, S. Garbe [*Solid-State Electron.* 12, 893 (1969)] measured 3×10^{14} Cs/cm² for optimum Cs coverage, and J. J. Uebbing and L. W. James [*J. Appl. Phys.* 41, 4505 (1970)] measured 5.6×10^{14} Cs/cm². Giving equal weight to these measurements, we determine a mean-optimum Cs coverage of 4.3×10^{14} Cs/cm². This is equivalent (within experimental accuracy) to one monolayer of Cs, since there are 4.43×10^{14} /cm² unit cells on the surface.

⁶L. W. James and J. L. Moll, *Phys. Rev.* 183, 740 (1969).

⁷High escape probabilities such as this were achieved with (110) GaAs surfaces. Our best yield curves obtained in this material are comparable to those obtained on (111B) GaAs by L. W. James, G. A. Antypas, J. Edgecumbe, R. L. Moon, and R. L. Bell, *J. Appl. Phys.* 42, 4976 (1971). Our yield is slightly better than theirs above 1.65 eV, but slightly lower than theirs below about 1.6 eV. The decreased yield in the infrared is probably due to the low doping of our material (1×10^{18} cm⁻³).

⁸L. W. James, J. L. Moll, and W. E. Spieer, 1968 *Proceedings of the Symposium on GaAs* (IPPS, London, 1969), p. 230.

⁹Since the settling of the Cs channel at the point of equilibrium (Cs loss \approx Cs gain) remains essentially constant at all exposure levels, it appears safe to assume that the sticking coefficient of Cs on $\text{InAs}_{0.4}\text{P}_{0.6}$ and on GaAs does not change significantly with coverage when the simultaneous-exposure technique of processing is used.

¹⁰Since the thickness of the low-work-function surface has such a profound effect on photoemission, it is not surprising that a great deal of progress in the processing of infrared cathodes has recently been made.

Section 3

HETEROCATHODE

3.0 CONCEPT OF THE HETEROCATHODE

The negative-electron-affinity photocathode such as GaAs-Cs₂O, owes its high efficiency to the fact that the electron barrier at the surface of the cathode is below the conduction-band minimum of the bulk material. This property is no longer preserved when semiconductor materials with bandgaps less than about 1.1 eV are used, and the efficiency of such cathodes declines very rapidly with decreasing bandgaps (as shown for example in Section 2.2). However, the potential 1.5 micron photocathode requires a smaller bandgap material so that efficient optical absorption can occur at this wavelength.

The small-bandgap requirement of the infrared cathode is thus at odds with the negative-potential-barrier requirement. Both requirements may be met however in a cathode which we shall term a heterocathode. This cathode consists of three distinct materials:

- (1) A small-bandgap material,
- (2) A large-bandgap material, and
- (3) A low-work-function-surface material.

A thin layer of the large-bandgap material is grown epitaxially on the small-bandgap material forming a heterojunction, (hence the name heterocathode) and a low-work-function material is deposited on the wide-bandgap material to give a negative electron-affinity.

The heterocathodes which we have attempted to investigate consist of a p-Ge:p-GaAs heterojunction and a Cs₂O low-work-function surface; and also a p-n Ge:p-GaAs homo-heterostructure again with a Cs₂O low-work-function surface. The energy level diagrams of these cathodes are shown in Figure 1 and Figure 2 respectively. In operation, the junctions are biased as shown.

Let us first consider the operation of the p-p Ge-GaAs heterostructure shown in Figure 1. In a reflective cathode, light is incident from the right. Photons with energy $E_{\text{photon}} \leq E_p < E_{\text{g, GaAs}}$ generate electron-hole pairs in the Ge. The photoelectrons diffuse to the interface, and are injected into the p-GaAs conduction band whence they diffuse into vacuum. Photons of energy $E_{\text{photon}} \geq E_{\text{g, GaAs}}$ are absorbed in both the GaAs and the Ge materials. Thus the spectral response of this cathode should extend from the ultraviolet through the visible and down to the bandgap of the Ge in the infrared.

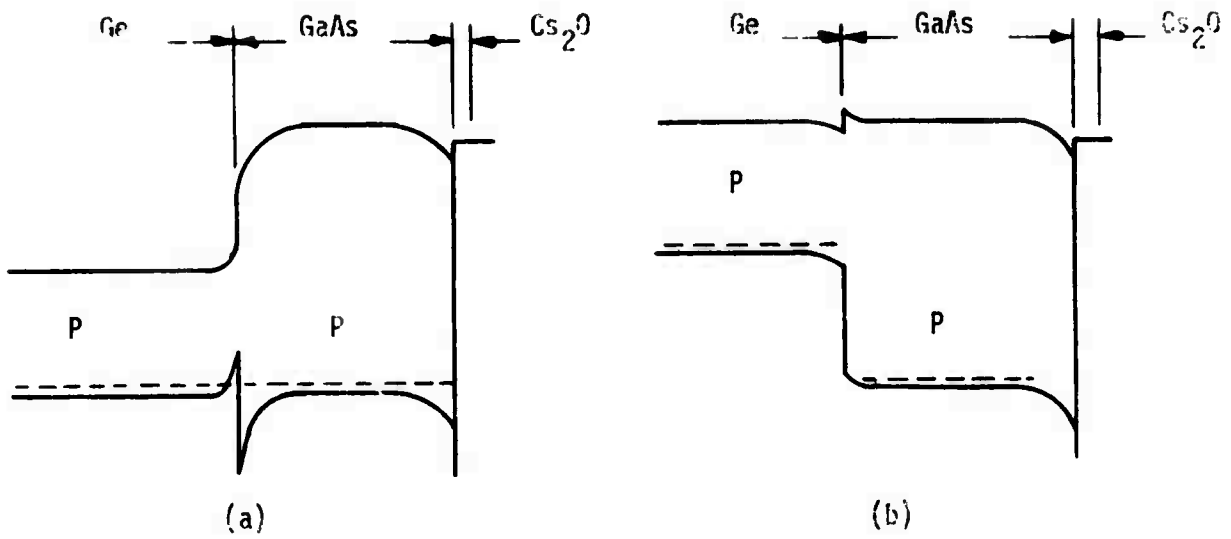


Figure 1. Ge:GaAs p-p Heterocathode-Energy-Level Diagram
(a) Unbiased, (b) Biased

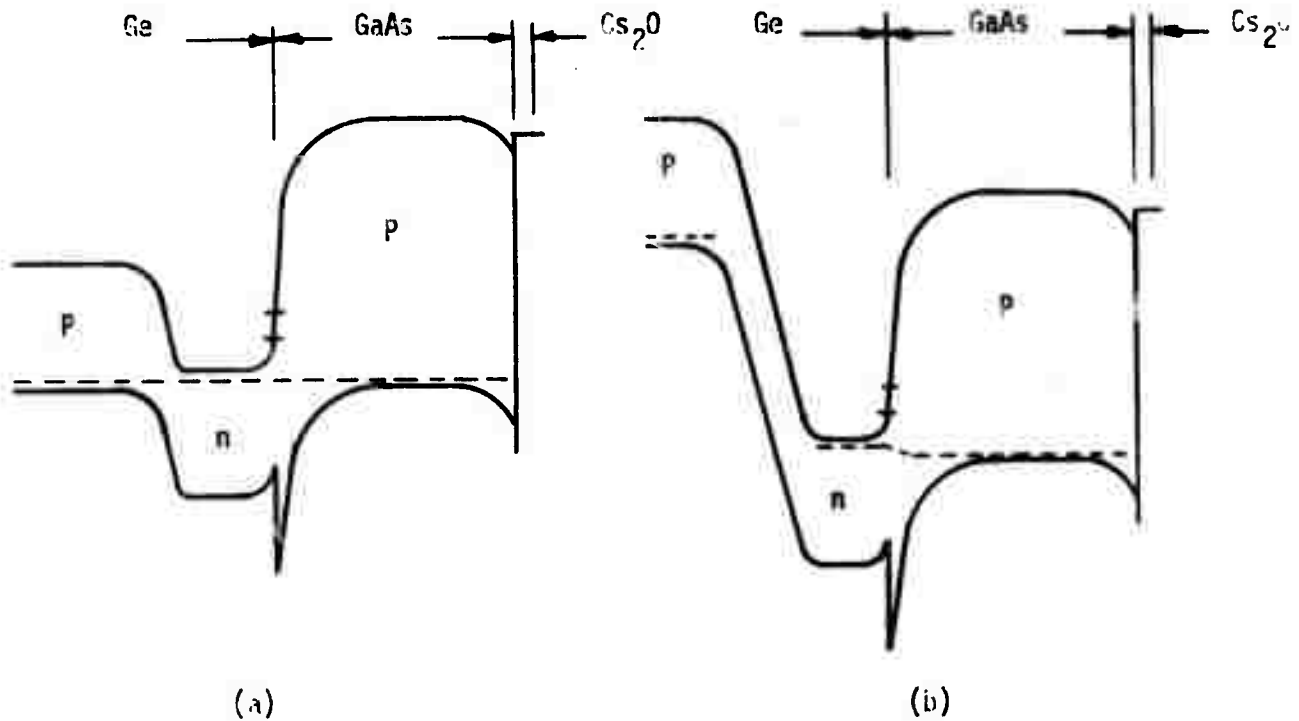


Figure 2. Ge pn:GaAs p Heterocathode-Energy-Level Diagram
(a) Unbiased, (b) Biased

3.0 (Continued)

Although we have maintained the desirable features of the negative-electron-affinity cathode in this approach, we have added complications which can have a very strong impact on the efficiency of the device. First, the injection efficiency for photoelectrons generated in the Ge and injected into the GaAs must be high. This is a controversial point, but let it suffice to say that an injection efficiency of about 60% has been measured⁽¹⁾ for a Ge-GaAs structure. Second, the injected electrons must diffuse through the GaAs to the surface before recombining. Thus the thickness of the GaAs layer should be less than the diffusion length. Since the diffusion length in the epitaxial layer is likely to be much less than that of bulk material, the thickness of the GaAs layer should probably not exceed about 0.3 micron. Finally, as shown in Figure 1(b) a forward bias is required to inject electrons from the Ge into the GaAs. The minimum amount of forward bias required is approximately equal to the valence band discontinuity, so that the forward hole current may or may not remain at an acceptable level. To avoid destroying the cathode, it may be necessary to pulse the bias, gating the detector on for short intervals.

The problems associated with a large forward hole current may be avoided by interposing a hole barrier between the p-Ge and the p-GaAs. This hole barrier may be n-Ge or n-GaAs or even a third semiconductor such as ZnSe which was proposed by Milnes and Feucht.⁽²⁾ The band diagram of such a cathode with an n-Ge hole barrier is shown in Figure 2. In operation, the device is biased as shown in Figure 2(b). Most of the voltage drop occurs across the back biased p-n Ge junction, and consequently the hole barrier is preserved even under high bias conditions.

The n-Ge layer must be made sufficiently thin so that a negligible fraction of the light is absorbed there and so that the photoelectrons generated in the p-Ge can be injected across the n region into the GaAs before recombining in the n-layer. Yet, it must be sufficiently thick to avoid tunneling problems. These considerations dictate that the n-layer should be on the order of 0.1 microns or less.

If these heterocathodes are to be operated in the transmission mode, the p-Ge material is subject to one further restriction: the thickness of the p-Ge layer must be less than or approximately equal to the electron diffusion-length in Ge. Since the maximum diffusion lengths in Ge are typically two orders of magnitude greater than in GaAs, one can easily envision a self-supporting transmission-heterocathode. In this report we confine ourselves to the reflective cathode.

3.1 Materials Growth

There are a number of different methods which can be used to grow GaAs on Ge. Our major concern in settling on a technique was that it be capable of high-quality growth at low temperatures and that the thickness of the grown layer could easily be controlled. Although GaAs had never been grown on Ge by the Gallium-Diethyl-Chloride (GDC) technique, we chose this method of chemical-vapor deposition since growth of GaAs on GaAs by this method had been reported down to 450°C. ⁽³⁾

In this technique, GDC, a colorless liquid which can be safely handled in air, is the Ga source. A 5% mixture of AsH₃ in H₂ was used for the As source, and diethyl zinc, ⁽⁴⁾ a pyrophoric liquid, was used for the Zn doping of the GaAs layers. A photograph of the growth apparatus is shown in Figure 3.

A vertical rf-heated, flow-type reactor, constructed of quartz, Teflon and stainless steel was used. The temperature of the pyrolytic graphite susceptor was monitored optically with a Raytek Infrared Thermometer, which was calibrated with a standard blackbody. The correct emissivity setting for the overall system was determined by observing the melting points of Ge and Zn under dynamic conditions.

The Ge substrates were largely mechanically polished and subsequently chemically polished for 10 minutes in a 3-1/2 HF:100 HNO₃ solution to remove the mechanical damage. One set of 30 polished substrates was purchased from the Semiconductor Processing Company. These substrates were prepared by the Sodium Hypochlorite technique, and were also etched for 10 minutes in 3-1/2 HF:100 HNO₃ just prior to growth.

Before growth, the substrates were thermally etched in the system at 750°C in H₂ for 5 minutes, whereupon the temperature was lowered to the growth temperature. The AsH₃ flow rate was typically 70 cc/min, and the H₂-GDC flow rate was approximately 420 cc/min. The diethyl zinc flow rates were approximately 11 cc/min for the sweep flow and about 1 cc/min for the bleed flow. The bleed flow rate quoted here could be in substantial error since it was very difficult to accurately calibrate the micrometer valve and the settings were not entirely reproducible for such a small flow rate.

The GaAs epitaxial layers were evaluated with the help of the apparatus shown in Figure 4. This setup includes the following measurement capabilities:

- (1) Photoluminescence
- (2) Copeland analyzer ⁽⁵⁾

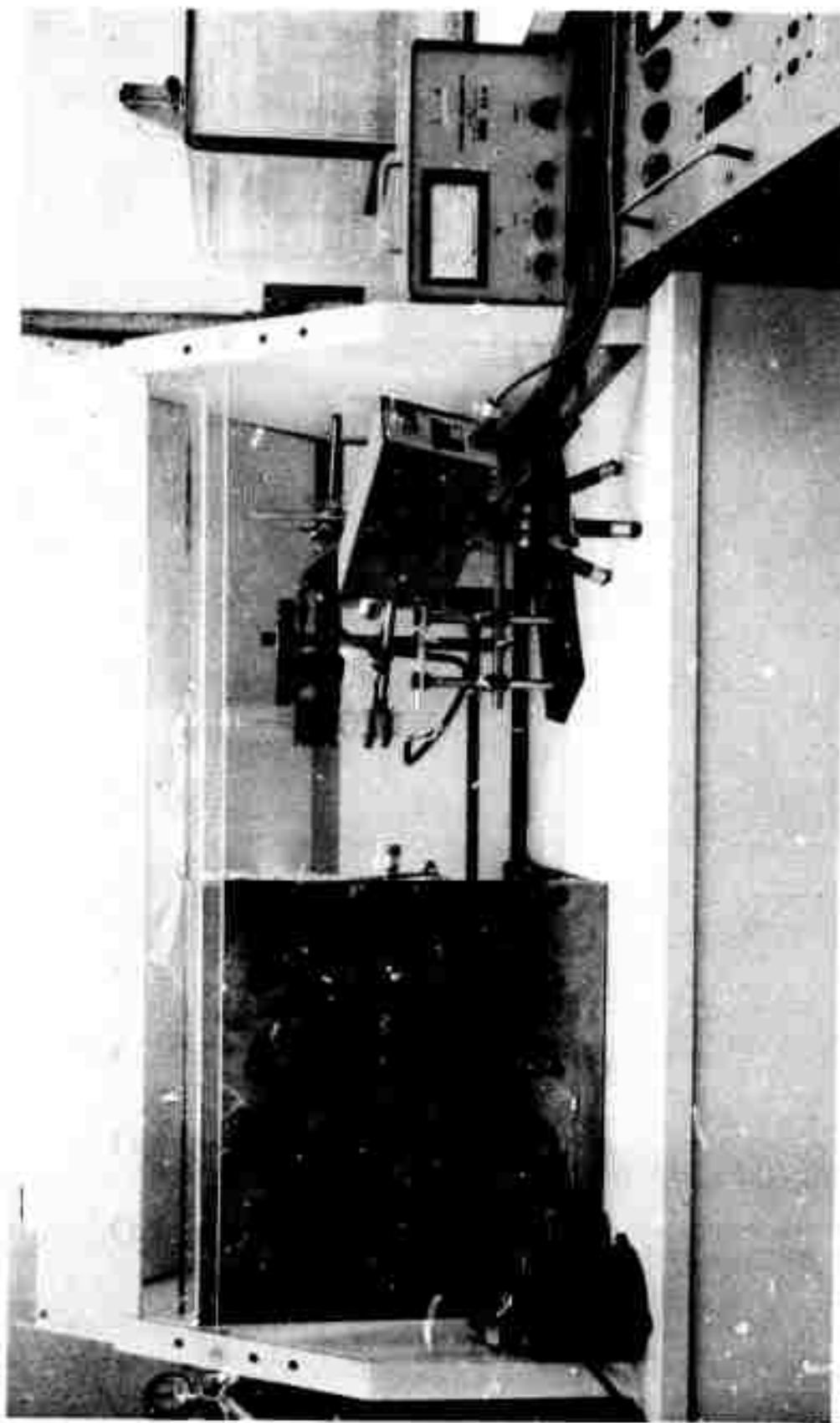


Figure 3. Photograph of Chemical Vapor Deposition Apparatus for the Growth of GaAs on Ge by the GDC technique

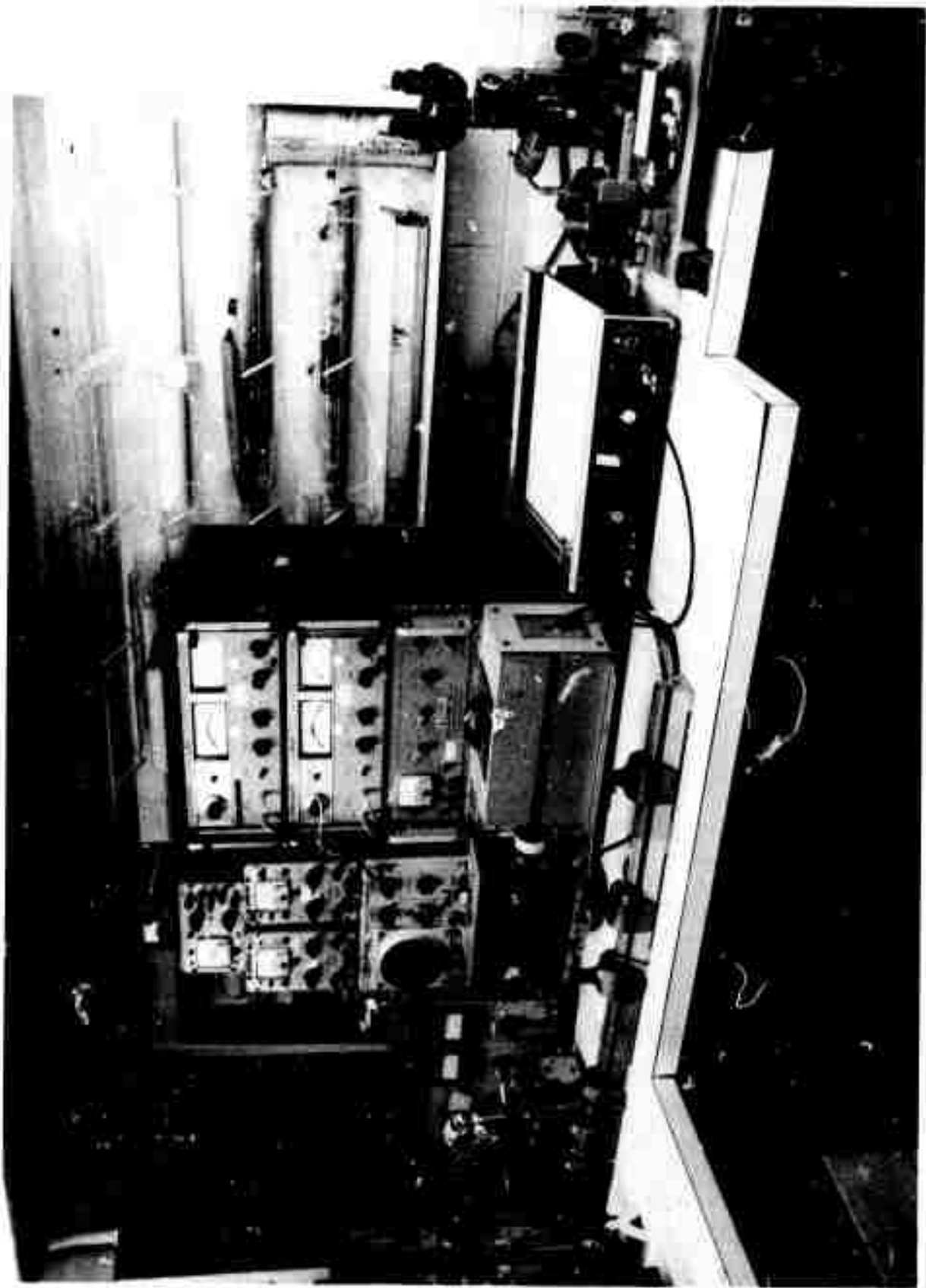


Figure 4. Measurement Apparatus Used to Characterize Grown Surfaces

3.1 (Continued)

- (3) Thermal probe
- (4) I-V characteristics.

The photoemission-measurement setup is shown in Figure 5.

Mirror smooth growth was obtained on either $\langle 111 \rangle$ or $\langle 100 \rangle$ Ge substrates misoriented by 5° at temperatures as low as 575°C . A photograph of a wire mesh reflected by a GaAs epitaxial layer grown on a $\langle 100 \rangle$ Ge substrate at 575°C is shown in Figure 6. The photographs shown in Figure 7 were taken at 100X magnification and give an even better indication of the quality of the surface achievable by this growth technique. Figure 7(a) shows the morphology of a GaAs surface grown at 575°C on a $\langle 111 \rangle$ Ge substrate. Except for the scratches due to the Ge substrate which are shown here so that the microscope could be focused, the surface shown in (a) is absolutely structureless. The pattern of streaks, running from northwest to southeast, is due to the microscope optics, as may be confirmed by comparing photographs (a), (c) and (d). For comparison, Figure 7(b) shows the growth obtained at 575°C on a $\langle 311 \rangle$ surface with no misorientation.

Figure 7(c) shows the growth obtained at 550°C on a $\langle 100 \rangle$ Ge substrate. Structure in the growth is beginning to appear at this temperature. At high temperature, the surface also begins to roughen. The photograph in Figure 7(d) shows the growth obtained at 675°C on a $\langle 111 \rangle$ Ge substrate.

The growth of GaAs by the GDC technique is a diffusion-controlled process. The growth rate is dependent on the total gas-flow, and it is independent of the substrate orientation. Furthermore, the growth rate, except at the temperature extremes, is essentially independent of temperature as shown in Figure 8. Diffusion controlled processes are generally encountered where flow conditions are unfavorable or where surface kinetics is rapid. We believe the latter to be the case in our growth.

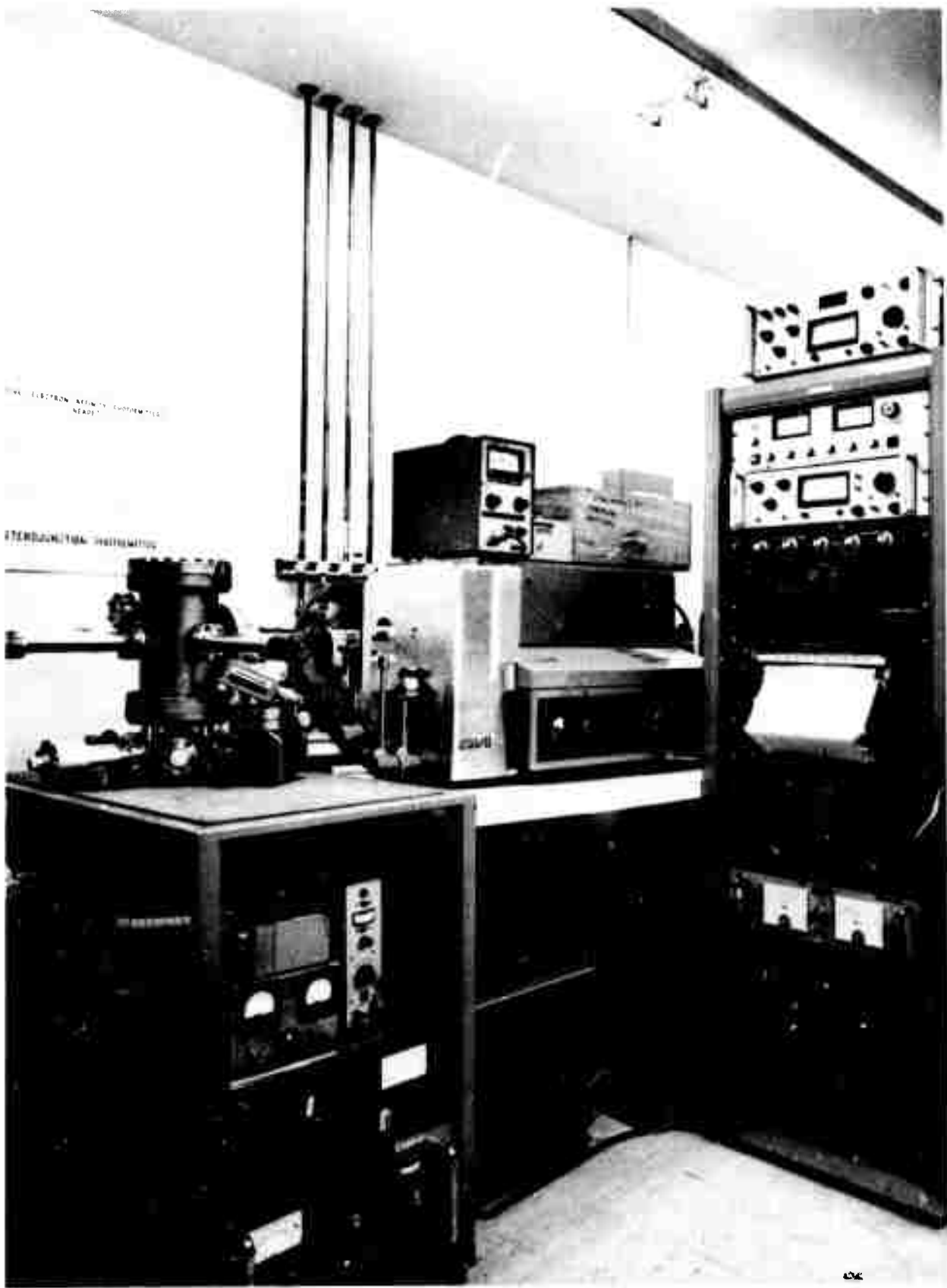


Figure 5. Automated-Photoemission-Measurement Setup

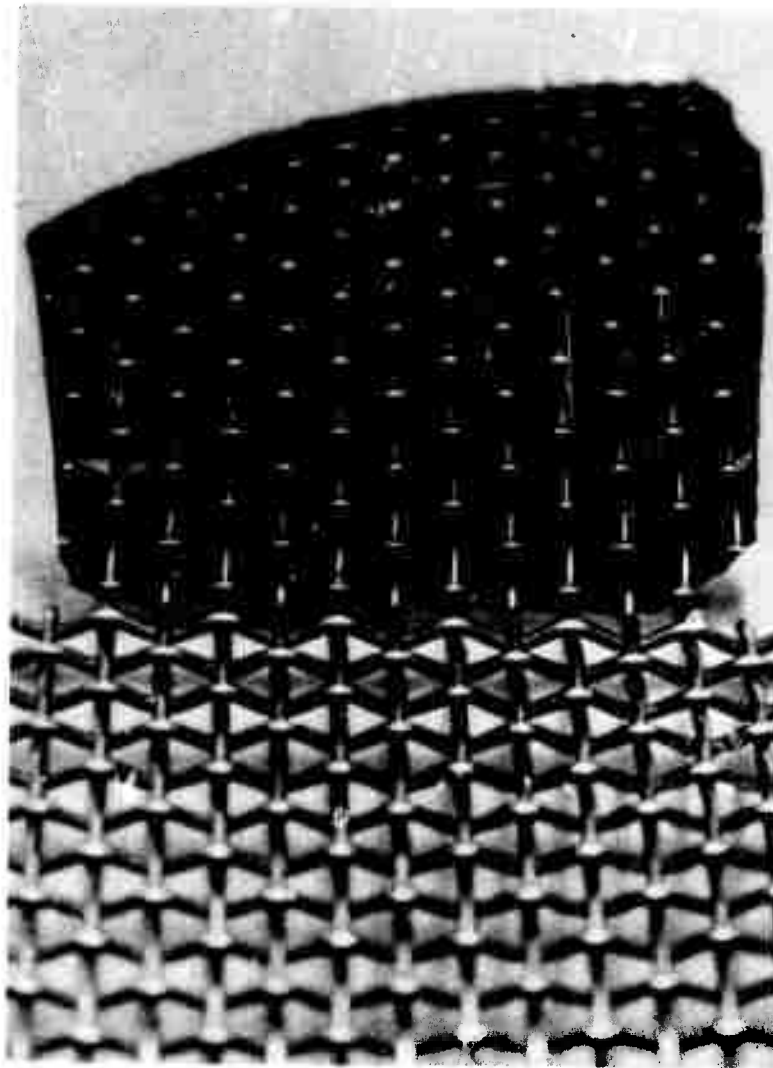


Figure 6. Photograph of a Wire Mesh Mirrored in a p-GaAs Epitaxial Layer Grown at 575°C on a $\langle 100 \rangle / 5^\circ$ Ge Substrate



(a)



(b)



(c)



(d)

Figure 7. Morphology of GaAs Epitaxial Growth on Ge, Shown at 100X Magnification and Grown on: (a) $\langle 111 \rangle / 5^\circ$ substrate at 575°C, (b) $\langle 311 \rangle$ substrate at 575°C, (c) $\langle 100 \rangle / 5^\circ$ substrate at 550°C, (d) $\langle 111 \rangle / 5^\circ$ substrate at 675°C

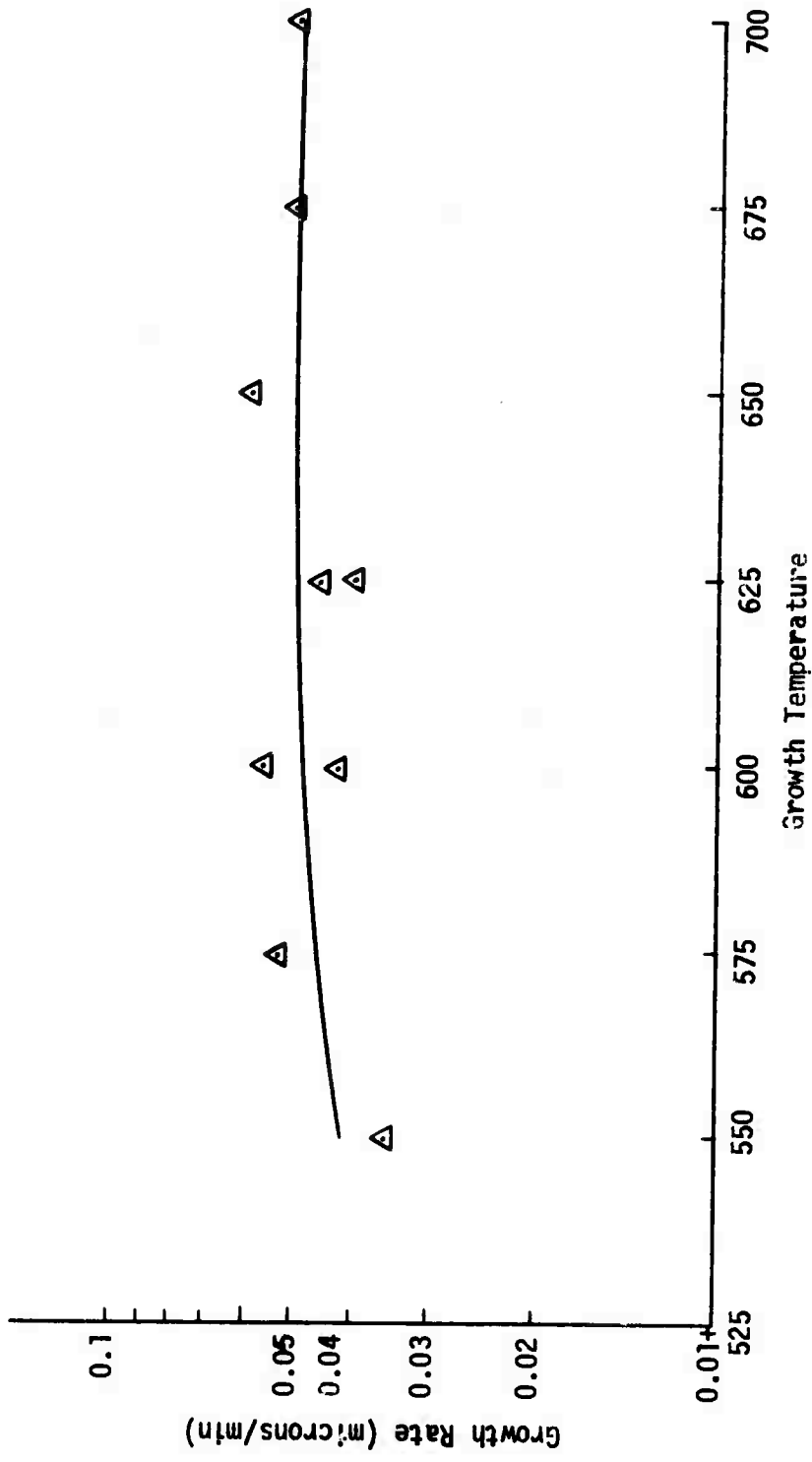


Figure 8. Temperature Dependence of Growth Rate

3.2 Heterojunction Devices

When GaAs is grown on Ge, As diffuses into the Ge substrate, generally converting the surface of a p-substrate to n-type Ge. If an n-type diffusion is being made into p-type material of concentration p , then a junction will occur where $n = p$. A solution of the diffusion equation for this case gives⁽⁶⁾

$$n_0 \left[1 - \operatorname{erf} \left(\frac{d}{2\sqrt{Dt}} \right) \right] = p \quad (1)$$

$$D = D_0 e^{-\Delta E/kT} \quad (2)$$

where $n_0 \text{ cm}^{-3}$ is the As surface concentration, $d \text{ cm}$ is the depth of the junction, $t \text{ sec}$ is the length of time of the diffusion, and $D \text{ cm}^2/\text{sec}$ is the diffusion constant as given by equation (2) with $\Delta E \text{ kcal/mole}$ the activation energy of As.

A summary of experimentally determined diffusion constants for As in Ge is given by Seeger et al.⁽⁷⁾ Using these data and equation (2) we calculate a diffusion constant $D \approx 1.1 \times 10^{-14} \text{ cm}^2/\text{sec}$ at 575°C . This is in good agreement with the results of Isawa⁽⁸⁾ who measured the diffusion of As into Ge during the epitaxial growth of GaAs. Using equation (2), we calculate from Isawa's data that $D = 1.7 \times 10^{-14} \text{ cm}^2/\text{sec}$.

From Isawa⁽⁸⁾ and from Schulze⁽⁹⁾ we determine that the As surface concentration is approximately 1×10^{19} . This is confirmed by our own measurements on $6 \times 10^{18} \text{ cm}^{-3}$ and $2 \times 10^{19} \text{ cm}^{-3}$ Ge substrates. The $6 \times 10^{18} \text{ cm}^{-3}$ Ge substrate surfaces convert to n-type during growth, whereas the $2 \times 10^{19} \text{ cm}^{-3}$ substrates do not. Thus, in order to make a p-p Ge-GaAs heterojunction when GaAs is grown on Ge, it is necessary to use very heavily doped p-Ge substrates with $p > 1 \times 10^{19} \text{ cm}^{-3}$. To fabricate the p-n Ge:p-GaAs structure shown in Figure 2, Ge substrates with $p < 1 \times 10^{19} \text{ cm}^{-3}$ must be used. No separate diffusion is required. The width of the n-region can be calculated from equation (1) and depends on the temperature at which the growth is made, and on the doping of the substrate. For example, for a 0.5-micron-thick growth at 575°C we get an n-layer thickness of 600 \AA and 1400 \AA for 10^{18} cm^{-3} and 10^{15} cm^{-3} substrate material respectively. Thus, the growth technique we have chosen is capable of satisfying the requirements of the heterocathode as outlined in Section 3.0.

We have found that the back surface of the Ge substrate also becomes n-type during growth. This n-layer was removed by etching in H_2O_2 under intense ultraviolet illumination. This is a selective etch for Ge. The function of the ultraviolet radiation is to increase the etch rate.

3.2 (Continued)

Ohmic contact to the Ge was made by the standard electroless-nickel-plating technique. The GaAs during this operation was protected by a film of AZ 135 OH Photoresist which was spun on at 3000 rpm.

After the Ni plating, the protective film was removed with acetone. Ohmic contact to the GaAs was made with a 2-4% Mn-Ag alloy⁽¹⁰⁾ evaporated in the vacuum system shown in Figure 9. Figure 10 is a photograph of a Ge-GaAs heterocathode slice showing the evaporated contact pattern on the GaAs surface. The slice is then diced into individual devices, one of which is shown in the photograph of Figure 11.

Rectification was observed in both directions for the p-n Ge-p GaAs heterocathode. This is expected since either the homojunction is backbiased or the heterojunction is backbiased, depending upon the polarity of the bias. For operation the p-n junction is backbiased as shown in Figure 2. Ten volts of back bias could repeatedly be supported by our devices made with 7 to $10 \times 10^{14} \text{ cm}^{-3}$ Ge. Thus the energy of photoelectrons generated in the p-Ge is well above that of the GaAs-conduction-band minimum.

We have also made photoemission measurements on these cathodes. At zero bias, the GaAs response was obtained, as would be expected. However, for any other bias condition, noise totally overpowered the signal, and it was not possible to make photoemission measurements. The noise may be due to contact problems, however, there was insufficient time to investigate this further. Consequently we could not measure the photoemission properties of this cathode beyond 0.9 micron.

It is the author's opinion, however, that photoemission out to 1.5 microns can be achieved by this technique. The growth and processing procedures outlined in this section appear well suited to the fabrication of a Ge:GaAs heterocathode. Since the electron injection efficiency from the Ge into the GaAs could not be measured, it is difficult to say what the efficiency at about 1.5 microns would be. One can make theoretical estimates, but the quantitative aspects of heterojunction calculations are in general not very precise, and the true evaluation of this concept must await further experimental investigation.

In future work, the noise problem should be investigated; the thickness of the n-Ge layer should be accurately measured; the heterojunction properties should be investigated, including factors affecting the injection efficiency; and extensive photoemission measurements should be made for different bias conditions.

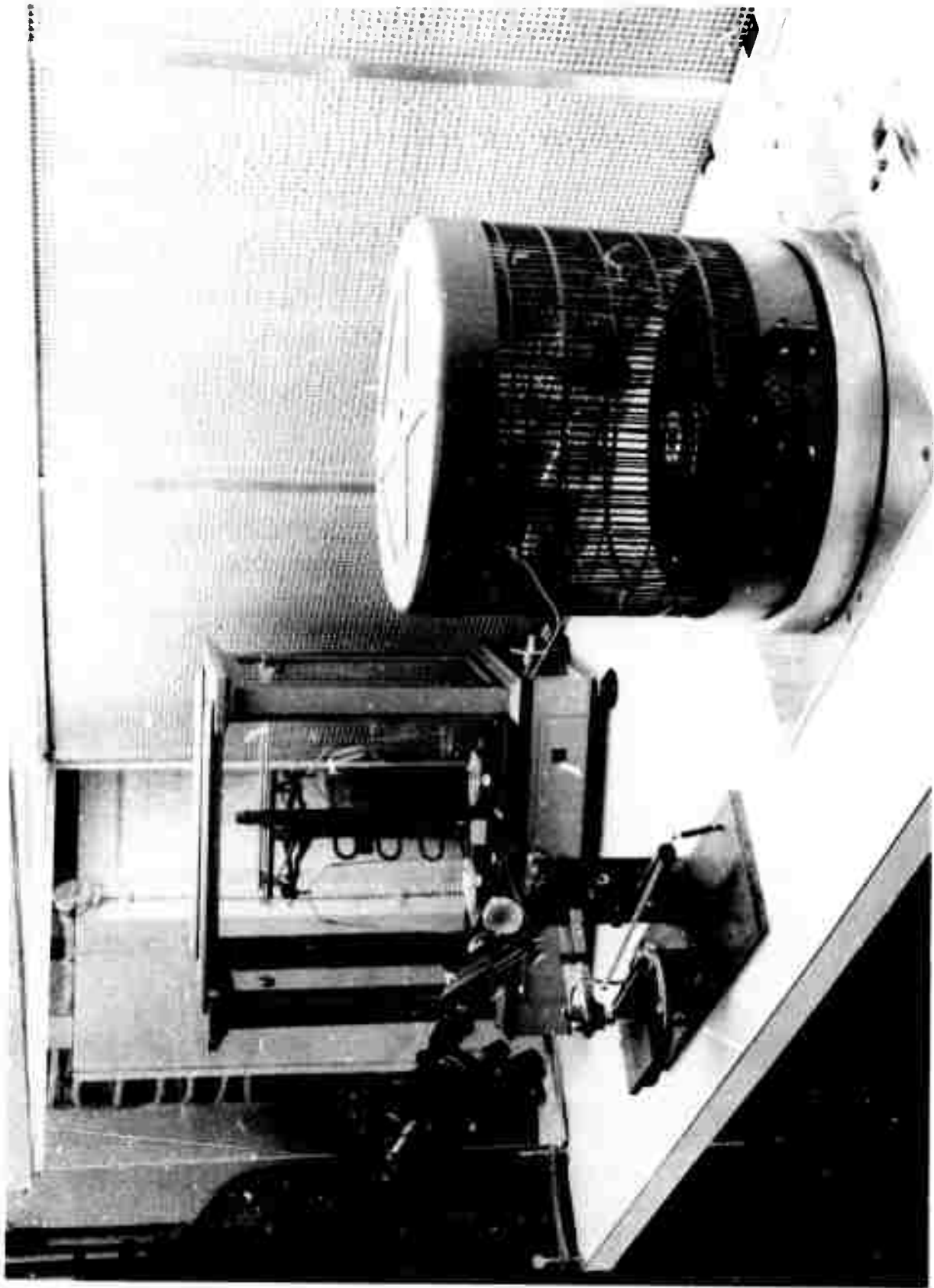


Figure 9. Vacuum Station Used to Make Ohmic Contacts to GaAs

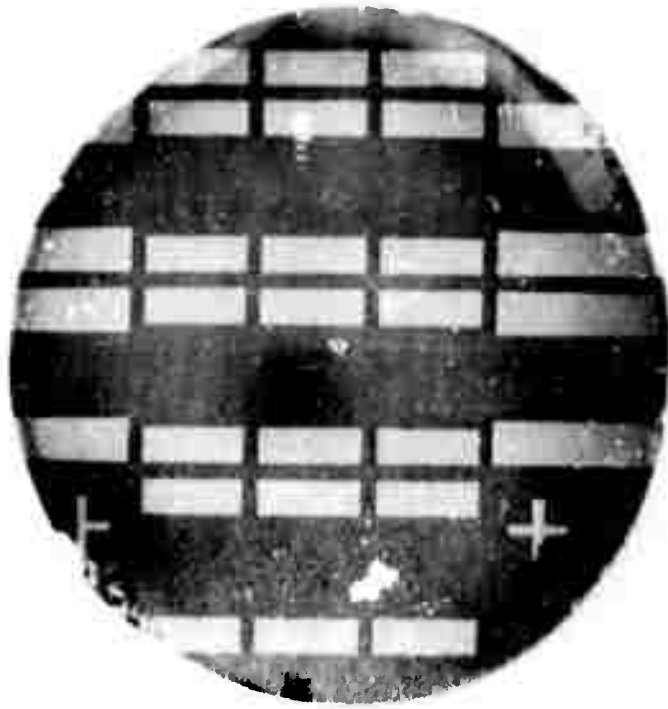


Figure 10. Photograph of Wafer with Ohmic-Contact Pattern on GaAs Surface

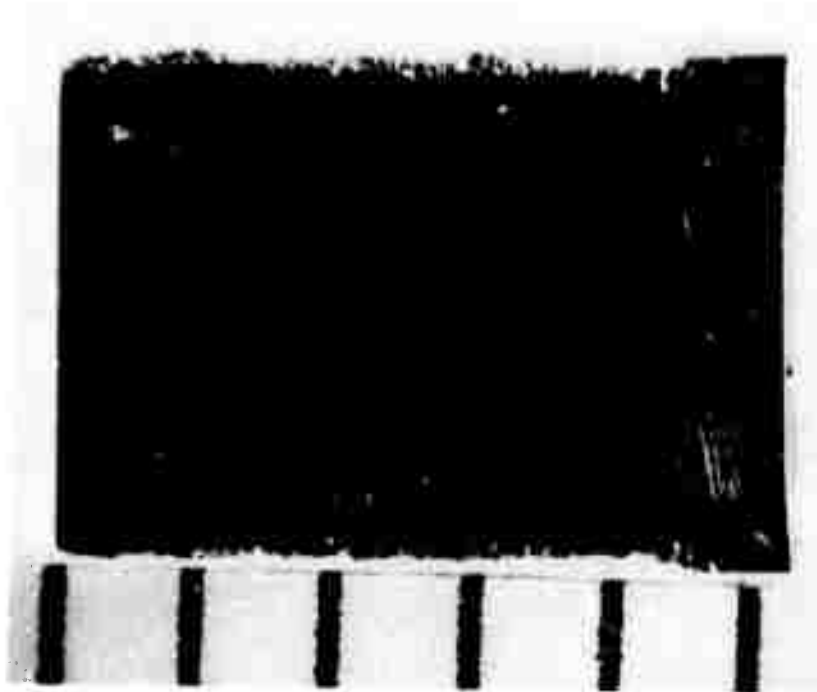


Figure 11. Photograph of One Device
The scale at the bottom of the picture is in millimeters.

REFERENCES

- (1) P. W. Kruse, F. C. Pribble, and R. G. Schulze, *J. Appl. Phys.* 38, 1718 (1967)
- (2) A. G. Milnes and D. L. Feucht, *Appl. Phys. Lett.* 19, 383 (1971)
- (3) K. Lindeke, W. Sack, and J. J. Nickl, *J. Electrochem. Soc.* 117, 1316 (1970)
- (4) R. W. Conrad and R. W. Haisty, *J. Electrochem. Soc.* 113, 199 (1966)
- (5) John A. Copeland, *IEEE Trans. Electron Devices*, ED-16, 445 (1969)
- (6) W. R. Runyon, *Silicon Semiconductor Technology*, McGraw-Hill Book Company, pp 199 (1965)
- (7) A. Seeger and K. P. Chik, *Phys. Status Solidi* 29, 455 (1968)
- (8) Nobuyuki Isawa, *Japan J. Appl. Phys.* 7, 81 (1968)
- (9) Richard G. Schulze, *J. Appl. Phys.* 37, 4295 (1966)
- (10) C. J. Nuese and J. J. Gannon, *J. Electrochem. Soc.* 115, 327 (1968)